This document is confidential and is proprietary to the American Chemical Society and its authors. Do not copy or disclose without written permission. If you have received this item in error, notify the sender and delete all copies.

"Backdoor Induction" of Chirality: Asymmetric Hydrogenation with Rh(I) Complexes of Triphenylphosphane Substituted ß-Turn Mimetics

Journal:	*Organometallics*
Manuscript ID:	om-2014-005385.R1
Manuscript Type:	Article
Date Submitted by the Author:	21-Jul-2014
Complete List of Authors:	Kirin, Srećko; Ruđer Boškovic Institute, Kokan, Zoran; Ruđer Boškovic Institute, Glasovac, Zoran; Ruđer Boškovic Institute, Majerić Elenkov, Maja; Ruđer Boškovic Institute, Gredičak, Matija; Ruđer Boškovic Institute, Jerić, Ivanka; Ruđer Boškovic Institute,

SCHOLARONE™
Manuscripts

"Backdoor Induction" of Chirality: Asymmetric Hydrogenation with Rh(I) Complexes of Triphenylphosphane Substituted β-Turn Mimetics

Zoran Kokan, Zoran Glasovac, Maja Majerić Elenkov, Matija Grdičak, Ivanka Jerić, and Srećko I. Kirin*

Ruđer Bošković Institute, Bijenička cesta 54, HR-10000 Zagreb, Croatia

Abstract.

Bioconjugate bidentate ligands **2**–**10** were obtained by tethering triphenylphosphane-carboxylic acid to amino acid substituted spacers with different flexibility, ranging from a rigid enediyne-based β-turn inducer to flexible linear aliphatic chains with up to eight carbon atoms. The 21 synthesized ligands revealed up to 81 % ee selectivity in rhodium catalyzed asymmetric hydrogenation of α,β-unsaturated amino acids. The key feature of the catalysts is the prochiral coordination sphere of the catalytic metal while the chirality is transmitted by "backdoor induction" form distant hydrogen-bonded amino acids. DFT calculations were applied to study the structure and relative stability of the precatalytic organometallic Rh(I) complexes, with particular emphasis on hydrogen bonded secondary structures.

Introduction.

β-Turns are among three main secondary structural motifs found in peptides and proteins.[1] Mimetics with turn-like structures are involved in various interactions between biomolecules,[2] therefore new scaffolds able to act as β-turn initiators are highly desirable. Generally, turn-like structures are known to be stabilized by the presence of conformational constrains, additional hydrogen bond donating and accepting groups or peptide bond *trans-cis* isomerization.[3–5]

A rather general model which may be used for efficient β-turn template screening is based on geometric analysis of the distances between C_α atoms in various β-turn fragments.[6] A cluster analysis of tetra-alanyl peptide segments, constructed by using torsion angles of different idealized β-turn types, identified clear patterns with triangle relationship (Chart 1a). We have reported that templates based on amino acids bridged with rigid *cis*-enediyne moiety have predefined turn-like conformation while maintaining enough flexibility to adjust upon addition of metal ions.[7] Moreover, the close resemblance with one class of β-turn geometry was found when applying geometric analysis on C_α surrogates in our templates (Chart 1b).

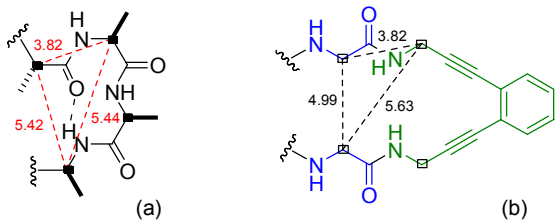

Chart 1. (a) Triangle relationship of C_α atoms (full squares) in a near-isosceles pattern found in β-turns;[5] (b) triangle relationship of C_α surrogates (hollow squares) in peptide mimetics described herein, calculated for the bis-*N*-acetyl derivative using B3LYP/6-31G(d); distances are given in (Å).

Recently, we have used triphenylphosphane amino acid bioconjugates as bioinspired monodentate ligands in Rh(I) catalyzed asymmetric hydrogenation of α,β-unsaturated amino acids.[8–12] Those [Rh(COD)(**Lig**)$_2$]BF_4 complexes feature a prochiral catalytically active metal; the chirality is transmitted by "backdoor induction" from distant hydrogen bonded amino acids (Chart 2).[8,13] Herein, we tether monodentate ligands to rigid or flexible linkers that allow different spatial arrangement of hydrogen bond donor and acceptor groups (of the amino acids) and as a consequence different phosphane - rhodium - phosphane bite angles,[14] and study the influence of the various linkers on the selectivity in asymmetric hydrogenation.

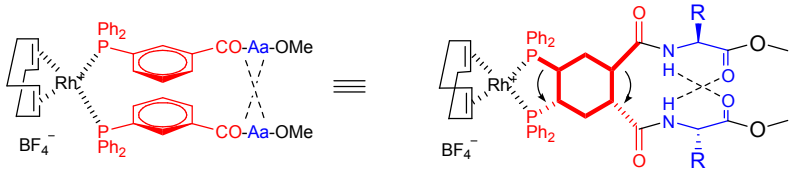

Chart 2. Side view (left) and top view (right) of *meta*-substituted [Rh(COD)(**Lig**)$_2$]BF_4 complexes. The upper central aromatic ring is indicated in bold; the arrows indicate the sign of helical chirality.

Results and Discussion.

Synthesis and characterization. Monodentate ligand amino acid bioconjugates **1A** and **1A$_p$** were prepared by standard peptide coupling in solution (TBTU/HOBt/DIPEA) reacting Boc-Ala-OH with *meta*- or *para*-substituted (diphenylphosphane)benzoic acid **I** or **II**, respectively (Scheme 1).[15]

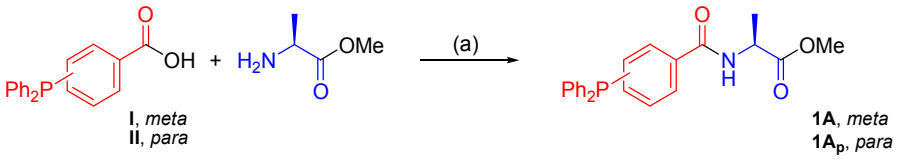

Scheme 1. *Reagents and conditions*: (a) Boc-Ala-OMe, TBTU/HOBt/DIPEA, DCM, r.t., 15h.

Bidentate ligand bioconjugates **2A** – **8A** and **4AA** – **5AA** were synthesized according to Scheme 2. First, the *N*-Boc protected derivatives **Boc-2A** – **Boc-8A** and **Boc-4AA** – **Boc-5AA** were prepared using two equivalents of Boc-Ala-OH and one equivalent of diamines NH_2-$(CH_2)_n$-NH_2 with different chain lengths, n = 2–8. In the second step, the Boc-derivatives were deprotected in standard conditions (TFA/DCM) and further coupled with *meta*-substituted triphenylphosphane-carboxylic acid **II** *via* the TBTU/HOBt/DIPEA protocol to give ligand amino acid or dipeptide bioconjugates **2A** – **8A** and **4AA** – **5AA**.

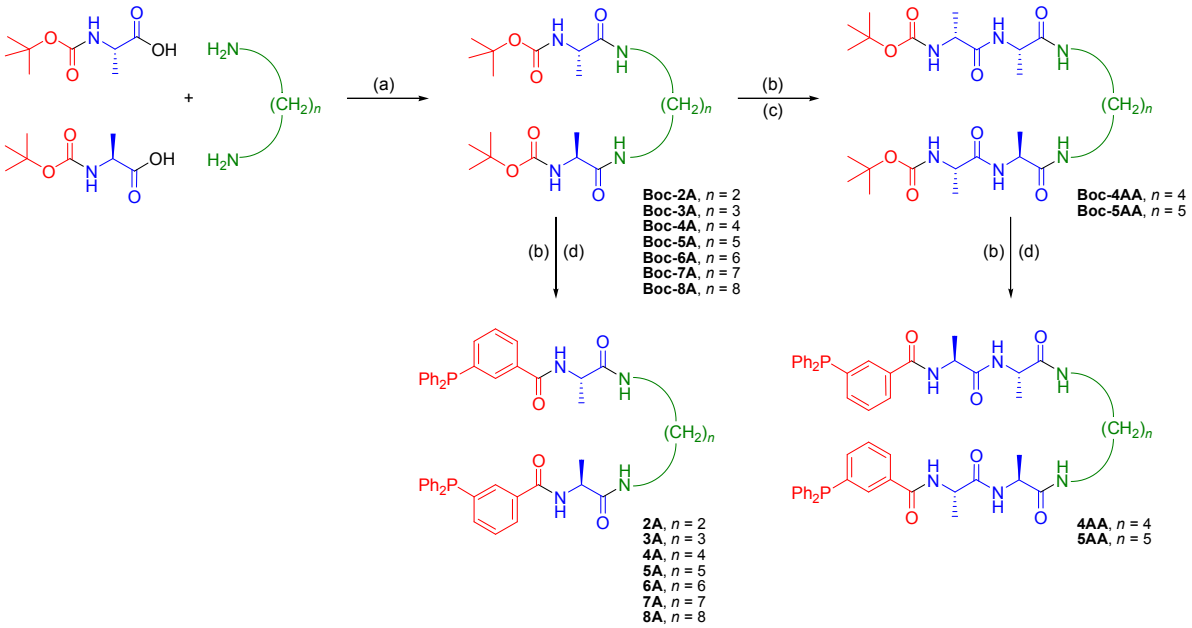

Scheme 2. *Reagents and conditions*: (a) TBTU/HOBt/DIPEA, DCM, r.t., 15h; (b) TFA/DCM (1:1); (c) Boc-Ala-OMe, TBTU/HOBt/DIPEA, DCM, r.t., 15h; (d) Ph_2P-*m*C_6H_4-CO_2H/TBTU/HOBt/DIPEA, DCM, r.t., 15h.

The synthesis of bidentate ligand bioconjugates **9** and **10** is highlighted in Scheme 3. Sonogashira coupling of alanine, leucine, valine or phenylalanine *N*-propargyl amides[16] and 1,2-diiodobenzene was performed in THF in the presence of piperidine, $Pd(PPh_3)_4$ and CuI to yield Boc-enediynes **Boc-9**. Catalytic hydrogenation of **Boc-9** using Pd/C in MeOH gave Boc-derivatives **Boc-10**. Ligand bioconjugates **9** and **10** were obtained by *N*-terminal deprotection of **Boc-9** and **Boc-10** (TFA/DCM), followed by coupling with triphenylphosphanes **I** or **II** in standard conditions (TBTU/HOBt/DIPEA).

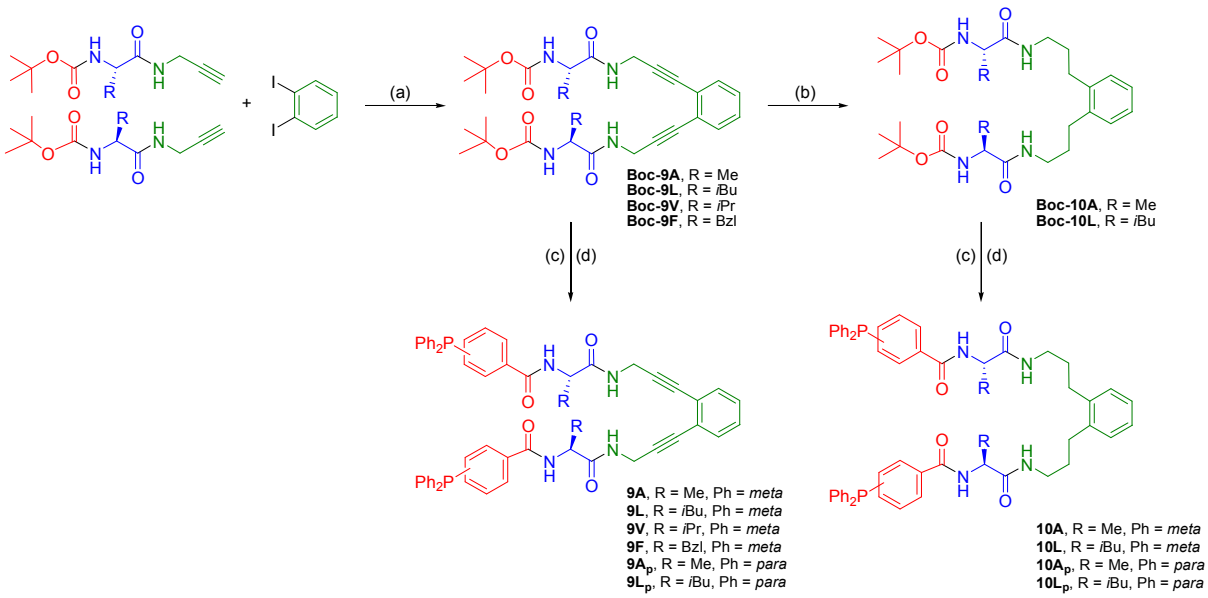

Scheme 3. *Reagents and conditions*: (a) piperidine (2 eq.), $Pd(PPh_3)_4$ (0.01 eq.) CuI (0.1 eq.) / THF; (b) Pd/C / MeOH; (c) TFA/DCM (1:1); (d) Ph_2P-C_6H_4-CO_2H/TBTU/HOBt/DIPEA, DCM, r.t., 15h.

Asymmetric Hydrogenation. Organometallic precatalyst complexes [Rh(COD)**Lig**]BF_4 with bidentate ligands, **Lig** = **2**–**10**, prepared *in situ* were used in asymmetric hydrogenation of α,β-unsaturated amino acids **S1** and **S2** (Scheme 4). Their catalytic activity was compared to *in situ* prepared complexes [Rh(COD)(**Lig**)$_2$]BF_4 with monodentate ligands, **Lig** = **1A** and $\mathbf{1A_p}$, the results are collected in Tables 1 – 2.

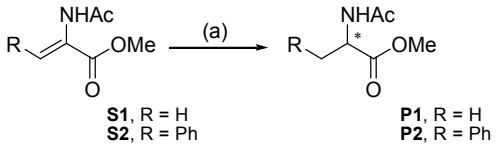

Scheme 4. *Reagents and conditions*: (a) [Rh(COD)**Lig**]BF_4 / H_2 / DCM (0.1 M substrate), r.t.; [Rh] : **Lig** : substrate = 1 : 1.1 : 100.

All examined Rh complexes proved to be efficient hydrogenation catalysts with excellent conversion of the substrate to product. Thus, optimal conditions for hydrogenation of **S1** are 2 h at r.t. and ambient pressure, while optimal condition for **S2** are 2 h at r.t. and elevated H_2 pressure (13 bar).

In particular, rigid enediyne ligands **9**, generally show higher selectivity than supramolecular ligand **1** or derivatives **10** with a more flexible linker. Best result with up to 81 % ee was obtained using the *meta*-substituted alanine ligand **9A** with a small side chain (Table 1, run 6). Catalysis with previously reported diphenlyphosphane-isophthalic acid based ligands also gave highest selectivity if alanine derivatives were used.[8a]

Table 1. Rh(I)-catalyzed asymmetric hydrogenation of **S1** or **S2** by using meta-substituted ligands **1**, **9** or **10**.[a]

Run	Ligand	Substrate	*t* [h]	*p* [bar]	Conv. [%][b]	*ee* (*R*) [%][c]
1	**1A/1A**	**S1**	2	1	> 98	56 (*S*) / 3 (*S*) [e]
2	**1A/1A**	**S2**	20	1	47	58 (*S*)
3	**1A/1A**	**S2**	2	13	> 98	61 (*S*)
4	**9A**	**S1**	2	1	> 98	75 / 56 [e]
5	**9A**	**S1**	2	1	> 98	73[d]
6	**9A**	**S2**	20	1	89	81
7	**9A**	**S2**	2	13	90	53
8	**9V**	**S1**	2	1	> 98	58
9	**9V**	**S2**	20	1	63	63
10	**9V**	**S2**	2	13	81	35
11	**9L**	**S1**	2	1	> 98	61
12	**9L**	**S2**	20	1	78	70
13	**9L**	**S2**	2	13	> 98	49
14	**9F**	**S1**	2	1	> 98	53
15	**9F**	**S2**	20	1	63	61
16	**9F**	**S2**	2	13	87	40
17	**10A**	**S1**	2	1	> 98	44
18	**10A**	**S2**	20	1	> 98	60
19	**10A**	**S2**	2	13	> 98	16
20	**10L**	**S1**	2	1	> 98	45
21	**10L**	**S2**	20	1	> 98	36
22	**10L**	**S2**	2	13	> 98	7

[a] Reaction according to Scheme 4. [b] Determined by ^{1}H NMR spectroscopic analysis. [c] Determined by GC analysis, BetaDex 225 for **S1**/**P1** and L-chirasil-Val for **S2**/**P2**. [d] Reaction performed at -5 °C. [e] MeOH was used as solvent.

A significant difference in selectivity was obtained for *meta*- and *para*-substituted ligands. *Meta*-substituted ligands **9** and **10** revealed moderate to good selectivity, mostly above 50 % ee for both substrates. On the contrary, for all *para*-substituted ligands $\mathbf{1A_p}$, $\mathbf{9A_p}$, $\mathbf{9L_p}$, $\mathbf{10A_p}$, and $\mathbf{10L_p}$, the selectivity in catalysis was generally below 20% ee (see Table S1, supplement). The favorable displaced stacking of the central aromatic rings in *meta*-substituted ligands, see (i) in Chart 3, can be used to explain the significantly higher selectivity in catalysis, as opposed to the less favorable face-to-face stacked aromatic rings in the *para*-substituted ligands, (ii) in Chart 3.[17]



Chart 3. Different stacking of the central aromatic rings: (i) *meta*- and (ii) *para*-substitution pattern. The lower ring is indicated with a dashed line.

The opposite stereochemical outcome of the catalytic reaction was obtained for *meta*-substituted bidentate ligands **9** and **10**, if compared to monodentate ligand **1A** (Table 1). Using monodentate ligand **1A**, the catalysis resulted in up to 61% ee in favor of (*S*)-**P1** or (*S*)-**P2**; this result is in agreement with our previous stereochemical analysis.[8b,13] However, if *meta*-substituted bidentate ligands **9** and **10** are used, an excess of (*R*)-**P1** or (*R*)-**P2** is obtained in catalytic hydrogenation.

Next, in an attempt to investigate the importance of structural rigidity in catalysis, instead of the rigid enediyne (in ligands **9**), aliphatic chains with varying length (up to eight carbon atoms) were incorporated in bidentate phosphane ligands **2A** – **8A**. *Meta*-substitution of the ligand and amino acid building block alanine were retained, because *meta*-substituted alanine ligands were the most selective catalyst so far. In the **2A** – **8A** series of ligands, highest selectivity in the studied asymmetric hydrogenation was 72% ee (*R*) for the optimal spacer length of $n = 5$ (Table 2, entry 10). Adding one amino acid per chain in **4AA** and **5AA** did not improve the selectivity (Table 2, entries 22 – 27). Interestingly, for a series of ligands **8A**, **10A** and **9A**, all with an 8 carbon atom spacer, the selectivity significantly increases upon constraining the spacer by means of a phenyl ring and/or triple bonds (Chart 4), indicating that complexes with rigid spacers give more structurally defined intermediates in the catalytic cycle.

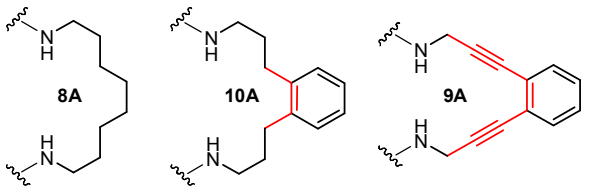

Chart 4. Spacers incorporated in ligands **8A**, **10A**, and **9A** compared to the selectivity obtained in catalysis of **S1** (upper row) or **S2** (lower row). Constrained carbon atoms are highlighted in red color

At ambient pressure, selectivity of the catalysts for both **S1** and **S2** is mostly similar, often with a slightly higher ee's in asymmetric hydrogenation of **S2**. Catalysis under increased hydrogen

pressure resulted in significant decrease of selectivity for **S2** using bidentate *meta*-ligands **9** and **10**, while it had almost no effect on *para*-ligands (Table S1). Monodentate ligand **1A** (Table 1, entries 2 and 3) exhibited only a slight change in selectivity for **S2** at higher pressure, which is in accordance with our previous work.[8a] Ligands with an alkyl spacer reveal an increase of selectivity with **3A** and **8A** (Table 2, entries 5, 6 and 20, 21), and an inversion of selectivity with **6A** (Table 2, entries 14, 15).

Table 2. Rh(I)-catalyzed asymmetric hydrogenation of **S1** or **S2** by using ligands **2**-**8**.[a]

Run	Ligand	Substrate	*t* [h]	*p* [bar]	Conv. [%][b]	*ee* (*R*) [%][c]
1	**2A**	**S1**	2	1	> 98	8
2	**2A**	**S2**	20	1	92	1
3	**2A**	**S2**	2	13	> 98	4
4	**3A**	**S1**	2	1	> 98	22
5	**3A**	**S2**	20	1	> 98	8
6	**3A**	**S2**	2	13	> 98	24
7	**4A**	**S1**	2	1	> 98	51 / 8 [d]
8	**4A**	**S2**	20	1	> 98	47
9	**4A**	**S2**	2	13	> 98	19
10	**5A**	**S1**	2	1	> 98	65
11	**5A**	**S2**	20	1	> 98	72
12	**5A**	**S2**	2	13	> 98	39
13	**6A**	**S1**	2	1	> 98	16
14	**6A**	**S2**	20	1	> 98	22
15	**6A**	**S2**	2	13	> 98	12 (*S*)
16	**7A**	**S1**	2	1	> 98	48
17	**7A**	**S2**	20	1	> 98	55
18	**7A**	**S2**	2	13	> 98	6
19	**8A**	**S1**	2	1	> 98	13 (*S*)
20	**8A**	**S2**	20	1	> 98	9 (*S*)
21	**8A**	**S2**	2	13	> 98	23 (*S*)
22	**4AA**	**S1**	2	1	> 98	29 (*S*)
23	**4AA**	**S2**	20	1	> 98	22 (*S*)
24	**4AA**	**S2**	2	13	> 98	12 (*S*)
25	**5AA**	**S1**	2	1	> 98	39
26	**5AA**	**S2**	20	1	> 98	48
27	**5AA**	**S2**	2	13	> 98	23

[a] Reaction according to Scheme 4. [b] Determined by ^{1}H NMR spectroscopic analysis. [c] Determined by GC analysis, BetaDex 225 for **S1**/**P1** and L-chirasil-Val for **S2**/**P2**. [d] MeOH was used as solvent.

Upon changing the solvent from dichloromethane to methanol (Tables 1 and 2), the quantitative yield of the catalytic hydrogenation is retained, while the selectivity decreases. In the case of ligands **1A** and **4A**, the selectivity is completely lost: 56 % to 3 % ee (Table 1, entry 1) and 51 % to 8 % ee (Table 2, entry 8), respectively. However, if **9A** is used as ligand in Rh(I) catalyzed hydrogenation, moderate selectivity is retained (Table 1, entry 4, 75 to 56 % ee). These results reveal the importance of hydrogen bonds for inducing selectivity, as shown in our previous work.[8a]

Precatalyst Rh(I) complexes, spectroscopy. Rh(I) complexes with ligands **1-10**, with 2:1 phosphorus donor to metal stoichiometry, were prepared *in situ* and studied by NMR and CD spectroscopy. The absence of amide proton resonances below δ = 7 ppm in ^{1}H NMR spectra of

Rh(I) complexes in a non-hydrogen bonding solvent ($CDCl_3$) indicates the involvement of amide protons in hydrogen bonding, suggesting an ordered structure of the metal complexes in solution (see Supporting Information). CD spectra of the Rh(I) complexes further support an ordered structure in CH_2Cl_2 solution, (Chart 5). In particular, CD signals of the Rh chromophore strongly support efficient "backdoor induction" of chirality from the chiral amino acids to the prochiral rhodium.[8,18–20]

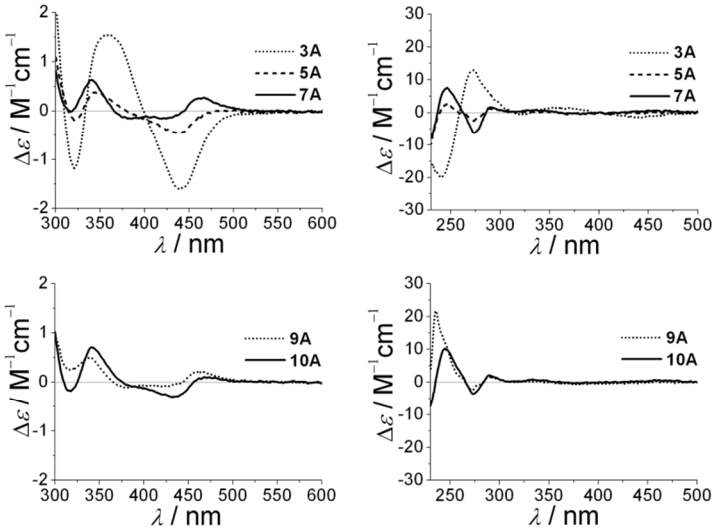

Chart 5. CD spectra of selected organometallic precatalytic complexes [Rh(COD)(**Lig**)]BF_4 in CH_2Cl_2.

Precatalyst Rh(I) complexes, computational study. Relative energies of Rh(I) precatalyst complexes were calculated using two theoretical methods. First, the widely accepted general purpose B3LYP approach was employed (**M1** method), which has been used earlier for investigation of the gas-phase chemistry of metal complexes.[21] The second calculation method **M2** using M06-L density functional is parameterized against a training set containing non-covalent interactions including π-π interactions and was recommended for calculation of metal complexes.[22]

In our study, supramolecular complexes with monodentate ligands $[Rh(COD)(\mathbf{1Lig})_2]^+$ as well as complexes with bidentate ligands $[Rh(COD)(\mathbf{9Lig})]^+$ were calculated; amino acid substituents were achiral glycine or chiral L-alanine. Geometry optimization of all investigated structures led to a square-planar rhodium coordination, as found in X-ray crystal structures of $[Rh(COD)(PPh_3)_2]^+$ derivatives.[23] Since the tetrafluoroborate anion does not coordinate to the metal, only the cations were calculated; the anion was left out for simplicity.

For each metal complex, several conformers based on different hydrogen bonding pattern between the two parallel amino acid strands were considered (Chart 6). The conformers can be distinguished by looking at the carbonyl oxygen atoms directly attached to the triphenlyphosphane moiety: The "Herrick conformer" (**a**) features both carbonyl oxygen atoms directly attached to the triphenlyphosphane moiety pointing outwards the cleft formed by the two amino acids. In the "van Staveren conformer" (**b**) one carbonyl oxygen atom points inwards the cleft and the other carbonyl oxygen points outwards, while in the "Gredičak conformer" (**c**) both carbonyl oxygen atoms point inwards. If the Bernstein-Davis classification is applied,[24] the

conformers differ in the number of atoms involved in the hydrogen-bonded rings: $R_2^2(10)$ for (**a**), $R_2^2(12)$ for (**b**), $R_2^2(14)$ for (**c1**) with inter-strand hydrogen bonds and an additional hydrogen bond with S(7) notation is possible in conformer (**b**). On the other hand, conformer (**c2**) contains two S(7) intra-strand hydrogen bonds.

The relative energies of the various conformers are collected in Table 3. Slightly different results with the two theoretical methods could be expected; our calculations show, however, that both methods predict the same trend of stabilities for the studied conformers.

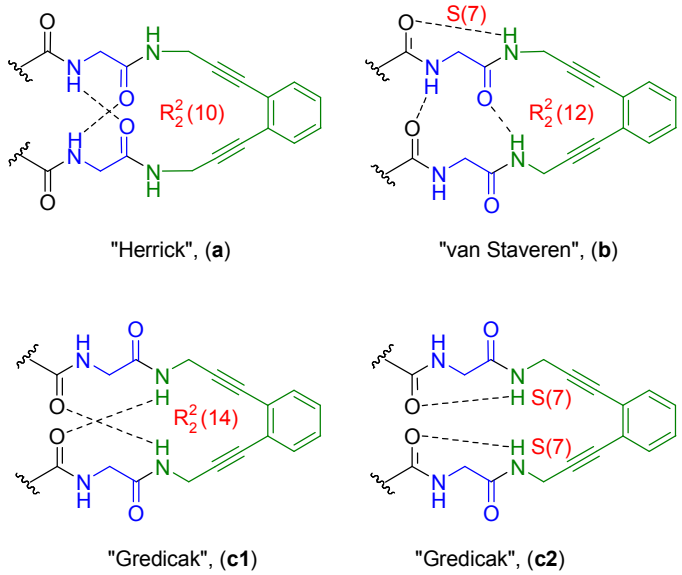

"Herrick", (**a**) "van Staveren", (**b**)

"Gredicak", (**c1**) "Gredicak", (**c2**)

Chart 6. Different hydrogen bonding patterns: Conformers (**a**), (**b**), (**c1**) and (**c2**) exemplified at the amino acid substituted enedyine backbone. Hydrogen bonds are indicated by dashed lines; Bernstein-Davis notation is indicated in red, according to ref. 24.

Table 3. Relative energies (E_{rel}) of several conformers of the achiral (**Lig**=G) and chiral (**Lig**=A) precatalytic complexes calculated using theoretical models **M1** and **M2**.[a]

			E_{rel} / kJ mol^{-1}		
			Lig=G	**Lig**=A	
	conf.			*M*-1,2'[b]	*P*-1,2'[b]
[Rh(COD)(**1Lig**)$_2$]$^+$	**a1**	**M1**	0.0	0.0	17.3
		(**M2**)	(0.0)	(0.0)	(5.4)
	a2	**M1**	8.4	28.0	12.3
		(**M2**)	(9.6)	(12.2)	(12.4)
	b	**M1**	25.0	30.6	37.9
		(**M2**)	(41.9)	(44.4)	(44.9)
[Rh(COD)(**9Lig**)]$^+$	**a1**	**M1**	0.0	0.0	30.9
		(**M2**)	(0.0)	(0.0)	(28.8)
	a2	**M1**	6.6	30.4	6.2
		(**M2**)	(4.7)	(25.5)	(13.1)
	b	**M1**	10.8	8.5	43.1
		(**M2**)	(28.2)	(26.3)	(46.9)

a) Relative energies (E_{rel}) were calculated by either B3LYP (**M1** model) or M06-L (**M2** model) density functional methods at the same optimized geometries. The most stable conformation was used as the reference structure; b) Configuration of the Rh metallacycle, see Chart 7 for explanation.

For the "Herrick conformer" two different substitution patterns of π – π stacked *meta*-disubstituted phenyl rings were considered: stretched conformer (**a1**) and crowded conformer (**a2**), (Chart 7). It is important to note, that the same helical chirality of the hydrogen bonded amino acid substituents, for example (*P*) in Chart 7, induces opposite chirality at the metal coordination sphere, (*M*) for (**a1**) and (*P*) for (**a2**). For the "van Staveren conformer" (**b**), geometrical optimization surprisingly predicts π – π stacking between one *meta*-disubstituted phenyl ring and one monosubstituted phenyl ring. "Gredičak conformer" (**c1**) with inter-strand hydrogen bonds was not identified as a minimum on the potential energy surface (PES). During optimization, inter-strand hydrogen bonds cleaved and intra-strand hydrogen bonds were established ending up in the (**c2**) conformer that is, however, 50 kJ mol^{-1} above the most stable conformer (**a1**). Additional attempts to optimize the (**c1**) conformer starting from (**c1**)-like initial geometries were not successful. Therefore, only conformers (**a**) and (**b**) were studied in detail, while the least stable conformer (**c2**) was abandoned.

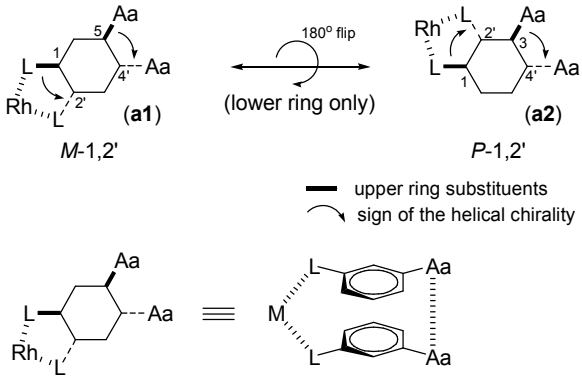

Chart 7. Different substitution pattern (**a1**) and (**a2**) of the *meta*-disubstituted rings in the Rh(I) complexes.[25] For a detailed stereochemical analysis see Supporting information.

Achiral supramolecular complex [Rh(COD)(**1G**)$_2$]$^+$ was studied first (Table 3). In this case, the conformers differ in the number of hydrogen bonds: conformers (**a1**) and (**a2**) each contain two hydrogen bonds, while conformer (**b**) has one such bond. Both applied theoretical models **M1** and **M2** predicted "Herrick conformer" (**a1**) to be the most stable (Table 3). The highest stability of "Herrick conformer" (**a**) is expected, since this conformer is found in the single crystal of [Pt(**1VA**)$_2$Cl$_2$],[9d] and (**a**) is also present in the ferrocene peptides.[13,26] However, while (**a1**) is significantly more stable than (**b**), (ΔE_{rel} > 25 kJ mol^{-1}, the relative energies of the crowded conformer (**a2**) are rather close to (**a1**), ΔE_{rel} = 6.6 (**M1**) and 4.7 kJ mol^{-1} (**M2**), (Table 3).

Next, achiral macroyclic complex [Rh(COD)(**9G**)]$^+$ was calculated. Including the β-turn mimicking building block introduces two more amide protons capable of hydrogen bonding. Again, the conformers differ in the number of hydrogen bonds: conformer (**a1**) and (**a2**) contains two hydrogen bonds each, and conformer (**b**) has three H bonds. The results obtained reveal that "Herrick conformer" (**a1**) is the most stable for [Rh(COD)**(9G)]**$^+$ as well, followed by (**a2**) and (**b**), but the energy difference between (**a1**) and (**b**) is only 10.8 kJ mol^{-1} (by **M2**), (Table 3).

Complexes [Rh(COD)(**1A**)$_2$]$^+$ and [Rh(COD)(**9A**)]$^+$ containing chiral amino acid alanine have also been calculated. In these chiral derivatives, inter-strand hydrogen bonding between the two amino acids induces helical chirality at the stacked phenyl rings, leading to different

stereoisomers (Table 3). The trends found for achiral glycine derivatives apply also for chiral alanine analogues: (i) "Herrick conformers" (**a**) are more stable than the "van Staveren" conformers (**b**) and (ii) the difference between (**a**) and (**b**) is larger for the supramolecular complex $[Rh(COD)(\mathbf{1A})_2]^+$ than for the bidentate complex $[Rh(COD)(\mathbf{9A})]^+$. However, only small energetic differences were calculated for conformers with different helical chirality of the rhodium coordination sphere that would lead to opposite configuration of the product in catalysis. For the chiral supramolecular complex $[Rh(COD)(\mathbf{1A})_2]^+$ ΔE_{rel} between 1,2'-*M* (**a1**) and 1,2'-*P* (**a1**) is only 5.4 kJ mol^{-1} (by **M2** theoretical model). In addition, for chiral bidentate complex $[Rh(COD)(\mathbf{9A})]^+$, three conformers of different helical chirality are found to be within 10 kJ mol^{-1}: 1,2'-*P* (**a2**) and 1,2'-*M* (**b**) are only by 6.2 and 8.5 kJ mol^{-1} (using **M1** theoretical model) less stable than 1,2'-*M* (**a1**). From the small energy differences calculated for the studied conformers of precatalytic complexes, it is not possible to predict a general trend for the configuration of the preferred product in catalysis.

Conclusion.

Bidentate triphenylphosphane amino acid ligands **Lig** containing β-turn inducing linkers with different flexibility have been synthesized and characterized. Precatalytic organometallic rhodium(I) complexes $[Rh(COD)(\mathbf{Lig})]BF_4$ adopt an ordered structure in non-hydrogen bonding solvents, as shown by NMR and CD spectroscopy. The structure and relative stability of selected precatalytic complexes was studied by DFT calculations using two theoretical models B3LYP and M06-L, and showed that stretched "Herrick conformer" (**a1**) is the most stable, but the difference in stability to crowded "Herrick conformer" (**a2**) can be rather small, $\Delta E_{rel} < 10$ kJ mol^{-1}.

The rhodium complexes were used as catalysts in asymmetric hydrogenation of α,β-unsubstituted amino acids. Bidentate ligands described in this study yielded more selective catalysts than their monodentate analogues (61 % ee (*S*) with monodentate ligand **1A**). The nature of the linker in the bidentate ligands has a major influence on the selectivity in catalysis. In particular, enantioselectivities up to 81 % ee (*R*) were obtained with ligand **9A** containing the most favorable rigid enediyne linker. Within the series of ligands with different lengths of the flexible –NH-$(CH_2)_n$-NH– linker, the best result has been obtained with ligand **5A**, $n = 5$, 72 % ee (*R*). The presented catalysts are enzyme models where an artificial chiral β-turn serves as minimal but functional outer-coordination sphere that controls the chirality of the prochiral catalytic metal in asymmetric catalysis. Results obtained herein clearly show that the chiral information far away from the catalytic metal has a significant impact on enantioselectivity in the studied hydrogenation reaction.

It is important to point out that subtle changes to the architecture of our L-amino acid substituted ligands allow access to both isomers of the product in the studied catalytic hydrogenation: While monodentate ligand **1A** yields an excess of the (*S*)-product, introducing a linker in most selective bidentate ligands **9A** and **5A** results in predominant formation of the (*R*)-product. In order to explain this turnover in selectivity and predict the configuration of the major product in catalysis, detailed experimental and computational data on the recation mechanism are necessary.[12] Work along these lines is in progress in our laboratories.

Experimental section.

General Methods. Reactions were carried out in ordinary glassware and chemicals were used as purchased from commercial suppliers without further purification. Pure L-amino acids were used. Reactions were monitored by TLC on Silica Gel 60 F254 plates and detected with UV lamp (254 nm) or ninhydrin; compounds were purified using automated flash chromatography equipped with a UV detector (254 nm) and prepacked silica columns. For reactions at low temperature, a cryostat device was used.

Mass spectra were measured on a HPLC-MS system coupled with 6410 Triple-Quadrupole mass spectrometer, operating in a positive ESI mode. High resolution mass spectra were obtained on a MALDI TOF-TOF instrument using CHCA matrix. CD spectra were recorded on a spectropolarimeter in 1 cm quartz Suprasil cells. NMR spectra were obtained on spectrometers operating at 300.13 or 600.13 MHz for ^{1}H, 75.47 or 150.92 MHz for ^{13}C and 242.93 MHz for ^{31}P nuclei. Chemical shifts, δ (ppm), indicate a downfield shift from the internal standard, tetramethylsilane, TMS, for ^{1}H NMR and H_3PO_4 (85 %) for ^{31}P NMR, or residual solvent signal for ^{13}C NMR (77.16 ppm $CDCl_3$ or 39.52 ppm DMSO-d_6). Coupling constants, *J*, are given in Hz. Enantiomeric excess was determined on a gas chromatograph (FID detector) using chiral fused silica capillary columns Beta Dex 225 (30 m × 0.25 mm × 0.25 μm) or Permabond L-chirasil-Val (25 m × 0.25 mm).

Computational details. All calculations were performed using Gaussian09 program package.[28] Geometries were optimized using B3LYP hybrid density functional[29] in conjunction with the Ahlrichs's SVP basis set[30] for the first row elements and TZVP basis set for phosphorus while LanL2DZ effective core potential[31] was employed for rhodium. Electronic energies were recalculated using two different density functionals indicated throughout the text as the calculation models **M1** and **M2**. The first model (**M1**) encompasses B3LYP hybrid density functional in conjunction with LanL2DZ ECP for rhodium and TZVP basis set for other elements. Alternatively, model **M2** was constructed by choosing M06-L density functional[22], in combination with Pople's 6-311++G(3df,2p) (C, H, O, N and P) and LanL2DZ (Rh) basis sets. The nature of the stationary points was verified by vibrational analysis at the optimized geometries and no imaginary frequencies were obtained. Total energies (E_{tot}) were obtained by summing **M1** or **M2** electronic energies with zero-point vibrational energies (E_{ZPV}) without any scaling of the latter. Visualisation of the optimized structures was done by MOLDEN 5.0.[32]

Ligands.

Peptide coupling, general procedure. 5-(Diphenylphosphino)isophthalic acid, TBTU, HOBt and DIPEA were stirred at room temperature in DCM. After 1 h, amino acid or peptide was added to the reaction mixture and stirring was continued overnight (approximately 15 h). The reaction mixture was then washed with $NaHCO_3$ (sat., aq.), citric acid (10 %, aq.) and NaCl (sat., aq.), dried over Na_2SO_4, filtered, evaporated in vacuum and purified by automated flash chromatography on a prepacked silica column.

Boc-protecting group removal. The corresponding Boc-protected amino acid or peptide was dissolved in DCM–trifluoroacetic acid (1:1, 5 mL) and stirred for 2 h at room temperature. The volatiles were evaporated under reduced pressure and the viscous residue was dissolved in 15 mL

of DCM. The residual trifluoroacetic acid was neutralized with excess of DIPEA (0.5 mL). This solution was used for further peptide synthesis.

1A. 3-(Diphenylphosphino)benzoic acid (126.9 mg, 0.41 mmol), HOBt (53.39 mg, 0.40 mmol), TBTU (132.1 mg, 0.41 mmol), DIPEA (0.140 mL, 0.85 mmol), H-Ala-OMe × HCl (61.7 mg, 0.44 mmol), DCM (50 mL). Chromatography on silica (12 g), EtOAc/Hexane gradient (TLC: R_f = 0.60, EtOAc/Hexane = 1/1). Yield 109.1 mg (67 %). ^{1}H NMR (600,14 MHz, $CDCl_3$) δ/ppm: 1.48 (d, 3H, J = 7 Hz), 3.77 (s, 3H), 4.73–4.77 (m, 1H), 6.59 (d, 1H, J = 7 Hz), 7.29–7.42 (m, 12H), 7.76–7.78 (m, 2H). ^{13}C NMR ($CDCl_3$, 75.48 MHz) δ/ppm: 18.7 (β), 48.7 (α), 52.7 (OMe), 127.7 (4), 128.8 (d, $^3J_{CP}$ = 7 Hz, 3', 3''), 128.9 (d, $^3J_{CP}$ = 6 Hz, 5), 129.2 (4', 4''), 132.3 (d, $^2J_{CP}$ = 25 Hz, 2), 133.9 (d, $^2J_{CP}$ = 20 Hz, 2', 2''), 134.3 (d, $^3J_{CP}$ = 8 Hz, 3), 136.6, 136.6 (d, $^1J_{CP}$ = 11 Hz, 1', 1''), 136.8 (d, $^2J_{CP}$ = 15 Hz, 6), 138.7 (d, $^1J_{CP}$ = 13 Hz, 1), 166.6 (7), 173.7 (A1). ESI-MS (m/z): 392.2 (M + H^+, 100 %). MALDI-HRMS (m/z): calc. 392.1410 ($C_{23}H_{22}NO_3P$ + H^+), found 392.1402.

1A$_p$. 4-(Diphenylphosphino)benzoic acid (117.8 mg, 0.39 mmol), HOBt (43.1 mg, 0.32 mmol), TBTU (97.1 mg, 0.30 mmol), DIPEA (0.200 mL, 1.21 mmol), H-Ala-OMe × HCl (48.5 mg, 0.35 mmol), DCM (50 mL). Chromatography on silica (12 g), EtOAc/Hexane gradient (TLC: R_f = 0.46, EtOAc/Hexane = 1/1). Yield 84.1 mg (71 %). ^{1}H NMR (600,14 MHz, $CDCl_3$) δ/ppm: 1.51 (d, 3H, J = 7 Hz), 3.79 (s, 3H), 4.77–4.82 (m, 1H), 6.69 (d, 1H, J = 7 Hz), 7.29–7.37 (m, 12H), 7.74 (dd, 2H, J_1 = 8 Hz, J_2 = 1 Hz). ^{13}C NMR ($CDCl_3$, 150.92 MHz) δ/ppm: 18.8 (β), 48.7 (α), 52.7 (OMe), 127.1 (d, $^3J_{CP}$ = 6.5 Hz, 3, 6), 128.8 (d, $^3J_{CP}$ = 7 Hz, 3', 3''), 129.2 (4', 4''), 133.7 (d, $^2J_{CP}$ = 19 Hz, 2, 6), 134.0 (d, $^2J_{CP}$ = 20 Hz, 3, 5), 134.1 (4), 136.5 (d, $^1J_{CP}$ = 11 Hz, 1', 1''), 142.7 (d, $^1J_{CP}$ = 14 Hz, 1), 166.6 (7), 173.7 (A1). ^{31}P NMR ($CDCl_3$, 242.93 MHz) δ/ppm: –5.08. ESI-MS (m/z): 430.4 (M + K^+, 53 %). MALDI-HRMS (m/z): calc. 392.1410 ($C_{23}H_{22}NO_3P$ + H^+), found 392.1415.

2A. 3-(Diphenylphosphino)benzoic acid (133.2 mg, 0.43 mmol), HOBt (61.7 mg, 0.46 mmol), TBTU (134.5 mg, 0.42 mmol), DIPEA (0.145 mL, 0.88 mmol), **Boc-2A** (84.9 mg, 0.21 mmol), DCM (50 mL). Chromatography (DCM/MeOH gradient, TLC: R_f = 0.20, DCM:MeOH = 10:0.5). Yield: 76.7 mg (45 %). ^{1}H NMR ($CDCl_3$, 300.13 MHz) δ/ppm: 1.40 (d, 6H, J = 7 Hz), 3.20–3.30 (m, 2H), 3.42–3.54 (m, 2H), 4.48–4.57 (m, 2H), 6.82 (d, 2H, J = 7 Hz), 6.92 (t, 2H, J = 4 Hz), 7.24–7.35 (m, 22H), 7.69 (dt, 2H, J_1 = 7.5 Hz, J_2 = 1.5 Hz), 7.79 (dt, 2H, J_1 = 8 Hz, J2 = 1.5 Hz). ^{13}C NMR ($CDCl_3$, 150.92 MHz) δ/ppm: 18.3 (β), 39.6 (a), 49.9 (α), 127.6 (4), 128.8 (d, $^3J_{CP}$ = 7 Hz, 3', 3''), 128.9 (d, $^3J_{CP}$ = 5.5 Hz, 5), 129.2 (4', 4''), 132.7 (d, $^2J_{CP}$ = 25 Hz, 2), 133.9 (d, $^2J_{CP}$ = 19 Hz, 2'), 133.9 (d, $^2J_{CP}$ = 19 Hz, 2''), 134.0 (d, $^3J_{CP}$ = 8 Hz, 3), 136.6 (d, $^1J_{CP}$ = 11 Hz, 1'), 136.6 (d, $^1J_{CP}$ = 11 Hz, 1''), 136.8 (d, $^2J_{CP}$ = 14.5 Hz, 6), 138.8 (d, $^1J_{CP}$ = 13.5 Hz, 1), 167.3 (7), 173.5 (A1). ESI-MS (m/z): 801.3 (M + Na^+, 100 %). MALDI-HRMS (m/z): calc. 779.2910 ($C_{46}H_{44}N_4O_4P_2$ + H^+), found 779.2906.

3A. 3-(Diphenylphosphino)benzoic acid (137.1 mg, 0.45 mmol), HOBt (63.4 mg, 0.47 mmol), TBTU (141.3 mg, 0.44 mmol), DIPEA (0.145 mL, 0.88 mmol), **Boc-3A** (92.8 mg, 0.22 mmol), DCM (50 mL). Chromatography (DCM/MeOH gradient, TLC: R_f = 0.20, DCM:MeOH = 9.5:0.5). Yield: 107.9 mg (61 %). ^{1}H NMR ($CDCl_3$, 600.14 MHz) δ/ppm: 1.42 (d, 6H, J = 7 Hz), 1.64–1.68 (m, 2H), 3.09–3.14 (m, 2H), 3.42–3.47 (m, 2H), 4.58–4.63 (m, 2H), 6.78 (d, 2H, J = 7 Hz), 7.10 (t, 2H, J = 6 Hz), 7.27–7.35 (m, 22H), 7.74 (dt, 2H, J_1 = 7 Hz, J_2 = 1.5 Hz), 7.80 (dt, 2H, J_1 = 8 Hz, J2 = 1.5 Hz). ^{13}C NMR ($CDCl_3$, 150.92 MHz) δ/ppm: 18.4 (β), 29.0 (b), 37.1 (a),

49.8 (α), 127.6 (4), 128.8 (d, $^3J_{CP}$ = 7 Hz, 3', 3"), 128.9 (d, $^3J_{CP}$ = 6 Hz, 5), 129.2 (4', 4"), 132.7 (d, $^2J_{CP}$ = 26 Hz, 2), 133.9 (d, $^2J_{CP}$ = 20 Hz, 2'), 133.9 (d, $^2J_{CP}$ = 19 Hz, 2"), 134.1 (d, $^3J_{CP}$ = 8 Hz, 3), 136.6 (d, $^1J_{CP}$ = 11 Hz, 1', 1"), 136.8 (d, $^2J_{CP}$ = 14 Hz, 6), 138.7 (d, $^1J_{CP}$ = 13.5 Hz, 1), 167.3 (7), 173.0 (A1). ESI-MS (m/z): 793.3 (M + H^+, 100 %). MALDI-HRMS (m/z): calc. 793.3067 ($C_{47}H_{46}N_4O_4P_2 + H^+$), found 793.3071.

4A. 3-(Diphenylphosphino)benzoic acid (132.3 mg, 0.43 mmol), HOBt (62.8 mg, 0.46 mmol), TBTU (135.1 mg, 0.42 mmol), DIPEA (0.145 mL, 0.88 mmol), **Boc-4A** (92.8 mg, 0.22 mmol), DCM (50 mL). Chromatography (DCM/MeOH gradient, TLC: R_f = 0.18, DCM:MeOH = 10:0.5). Yield: 93.6 mg (54 %). ^{1}H NMR ($CDCl_3$, 300.13 MHz) δ/ppm: 1.29–1.42 (m, 4H), 1.43 (d, 6H, J = 7 Hz), 2.92–3.03 (m, 2H), 3.22–3.33 (m, 2H), 4.69–4.78 (m, 2H), 7.04 (d, 2H, J = 8 Hz), 7.08 (dd, 2H, J_1 = 6 Hz, J_2 = 5 Hz), 7.24–7.36 (m, 22H), 7.70 (dt, 2H, J_1 = 7.5 Hz, J_2 = 1.5 Hz), 7.79 (dt, 2H, J_1 = 8 Hz, J_2 = 1.5 Hz). ^{13}C NMR ($CDCl_3$, 150.92 MHz) δ/ppm: 18.8 (β), 26.4 (b), 39.2 (a), 49.5 (α), 127.4 (4), 128.8 (d, $^3J_{CP}$ = 7 Hz, 3', 3"), 128.8 (d, $^3J_{CP}$ = 6 Hz, 5), 129.1, 129.1 (4', 4"), 132.8 (d, $^2J_{CP}$ = 24.5 Hz, 2), 133.9 (d, $^2J_{CP}$ = 19 Hz, 2'), 133.9 (d, $^2J_{CP}$ = 20.5 Hz, 2"), 134.0 (d, $^3J_{CP}$ = 6 Hz, 3), 136.5 (d, $^1J_{CP}$ = 11 Hz, 1'), 136.6 (d, $^1J_{CP}$ = 10.5 Hz, 1"), 136.8 (d, $^2J_{CP}$ = 15 Hz, 6), 138.7 (d, $^1J_{CP}$ = 14 Hz, 1), 167.3 (7), 173.0 (A1). ^{31}P NMR ($CDCl_3$, 242.93 MHz) δ/ppm: –5.09. ESI-MS (m/z): 829.4 (M + Na^+, 43 %). MALDI-HRMS (m/z): calc. 807.3223 ($C_{48}H_{48}N_4O_4P_2 + H^+$), found 807.3227.

4AA. 3-(Diphenylphosphino)benzoic acid (104.7 mg, 0.34 mmol), HOBt (48.0 mg, 0.36 mmol), TBTU (105.6 mg, 0.33 mmol), DIPEA (0.150 mL, 0.91 mmol), **Boc-4AA** (91.1 mg, 0.16 mmol), DCM (50 mL). Chromatography (DCM/MeOH gradient, TLC: R_f = 0.26, DCM:MeOH = 9.5:0.5). Yield: 112.4 mg (69 %). ^{1}H NMR (DMSO-d_6, 600.14 MHz) δ/ppm: 1.18 (d, 6H, J = 7 Hz), 1.31 (d, 6H, J = 7 Hz), 1.33–1.35 (m, 4H), 2.93–2.99 (m, 2H), 3.01–3.06 (m, 2H), 4.18–4.23 (m, 2H), 4.39–4.43 (m, 2H), 7.24–7.27 (m, 8H) 7.29–7.32 (m, 2H), 7.39–7.42 (m, 12H), 7.48–7.50 (m, 2H), 7.70 (t, 2H, J = 5.5 Hz), 7.88–7.93 (m, 6H), 8.57 (d, 2H, J = 7 Hz). ^{13}C NMR ($CDCl_3$, 150.92 MHz) δ/ppm: 17.6, 18.3 (1,2β), 26.2 (b), 38.1 (a), 48.1, 49.2 (1,2α), 128.0 (4), 128.6 (d, $^3J_{CP}$ = 5 Hz, 5), 128.8 (d, $^3J_{CP}$ = 7 Hz, 3', 3"), 129.0, 129.1 (4', 4"), 132.7 (d, $^2J_{CP}$ = 26 Hz, 2), 133.2 (d, $^2J_{CP}$ = 20 Hz, 2'), 133.2 (d, $^2J_{CP}$ = 19.5 Hz, 2"), 134.2 (d, $^3J_{CP}$ = 8 Hz, 3), 135.6 (d, $^2J_{CP}$ = 14 Hz), 136.2 (d, $^1J_{CP}$ = 11 Hz, 1'), 136.2 (d, $^1J_{CP}$ = 11.5 Hz, 1"), 137.1 (d, $^1J_{CP}$ = 13 Hz, 1), 165.8 (7), 171.8 (1,2A1). ESI-MS (m/z): 949.4 (M + H^+, 100 %). MALDI-HRMS (m/z): calc. 949.3965 ($C_{54}H_{58}N_6O_6P_2 + H^+$), found 949.3981.

5A. 3-(Diphenylphosphino)benzoic acid (126.6 mg, 0.41 mmol), HOBt (60.0 mg, 0.44 mmol), TBTU (131.2 mg, 0.41 mmol), DIPEA (0.145 mL, 0.88 mmol), **Boc-5A** (94.6 mg, 0.21 mmol), DCM (50 mL). Chromatography (DCM/MeOH gradient, TLC: R_f = 0.21, DCM:MeOH = 9.5:0.5). Yield: 66.0 mg (39 %). ^{1}H NMR ($CDCl_3$, 600.14 MHz) δ/ppm: 1.16–1.21 (m, 2H), 1.40–1.49 (m, 4H), 1.45 (d, 6H, J = 7 Hz), 2.98–3.02 (m, 2H), 3.32–3.37 (m, 2H), 4.71–4.76 (m, 2H), 6.92 (dd, 2H, J_1 = 6.5 Hz, J_2 = 4 Hz), 7.21–7.33 (m, 24H), 7.69 (dt, 2H, J_1 = 8 Hz, J_2 = 1.5 Hz), 7.81 (dt, 2H, J_1 = 8 Hz, J_2 = 1.5 Hz). ^{13}C NMR ($CDCl_3$, 75.48 MHz) δ/ppm: 18.2 (β), 23.0 (c), 28.2 (b), 38.8 (a), 49.3 (α), 127.4 (4), 128.8 (d, $^3J_{CP}$ = 7 Hz, 3', 3"), 128.9 (d, $^3J_{CP}$ = 8 Hz, 5), 129.1 (4', 4"), 133.0 (d, $^2J_{CP}$ = 26 Hz, 2), 133.9 (d, $^2J_{CP}$ = 20 Hz, 2', 2"), 134.0 (d, $^3J_{CP}$ = 8 Hz, 3), 136.6 (d, $^1J_{CP}$ = 11 Hz, 1', 1"), 136.8 (d, $^2J_{CP}$ = 14 Hz, 6), 138.6 (d, $^1J_{CP}$ = 13.5 Hz, 1), 167.4 (7), 173.1 (A1). ^{31}P NMR ($CDCl_3$, 242.93 MHz) δ/ppm: –5.07. ESI-MS (m/z): 821.3 (M + H^+, 43 %). MALDI-HRMS (m/z): calc. 821.3380 ($C_{49}H_{50}N_4O_4P_2 + H^+$), found 821.3361.

5AA. 3-(Diphenylphosphino)benzoic acid (93.9 mg, 0.31 mmol), HOBt (47.6 mg, 0.35 mmol), TBTU (101.6 mg, 0.32 mmol), DIPEA (0.150 mL, 0.91 mmol), **Boc-5AA** (93.3 mg, 0.16 mmol), DCM (50 mL). Chromatography (DCM/MeOH gradient, TLC: R_f = 0.27, DCM:MeOH = 9.5:0.5). Yield: 92.8 mg (63 %). ^{1}H NMR (DMSO-d_6, 600.14 MHz) δ/ppm: 1.17–1.22 (m, 2H), 1.18 (d, 6H, J = 7 Hz), 1.31 (d, 6H, J = 7 Hz), 1.32–1.37 (m, 4H), 2.93–3.04 (m, 4H), 4.18–4.23 (m, 2H), 4.38–4.43 (m, 2H), 7.24–7.27 (m, 8H) 7.29–7.32 (m, 2H), 7.39–7.42 (m, 12H), 7.48–7.51 (m, 2H), 7.66 (t, 2H, J = 5.5 Hz), 7.89–7.93 (m, 6H), 8.58 (d, 2H, J = 7 Hz). ^{13}C NMR ($CDCl_3$, 75.48 MHz) δ/ppm: 17.6, 18.2 (1,2β), 23.5 (c), 28.6 (b), 38.4 (a), 48.1, 49.3 (1,2α), 128.0 (4), 128.6 (d, $^3J_{CP}$ = 5 Hz, 5), 128.8 (d, $^3J_{CP}$ = 7 Hz, 3', 3''), 129.1 (4', 4''), 132.7 (d, $^2J_{CP}$ = 26 Hz, 2), 133.2 (d, $^2J_{CP}$ = 19.5 Hz, 2'), 133.3 (d, $^2J_{CP}$ = 19.5 Hz, 2''), 134.2 (d, $^3J_{CP}$ = 8 Hz, 3), 135.7 (d, $^2J_{CP}$ = 14 Hz), 136.2 (d, $^1J_{CP}$ = 11 Hz, 1'), 136.2 (d, $^1J_{CP}$ = 11 Hz, 1''), 137.1 (d, $^1J_{CP}$ = 13 Hz, 1), 165.8 (7), 171.7, 171.8 (1,2A1). ESI-MS (m/z): 963.4 (M + H^+, 100 %). MALDI-HRMS (m/z): calc. 963.4122 ($C_{55}H_{60}N_6O_6P_2$ + H^+), found 963.4124.

6A. 3-(Diphenylphosphino)benzoic acid (148.0 mg, 0.48 mmol), HOBt (67.0 mg, 0.50 mmol), TBTU (154.0 mg, 0.48 mmol), DIPEA (0.160 mL, 0.97 mmol), **Boc-6A** (116.1 mg, 0.25 mmol), DCM (50 mL). Chromatography (DCM/MeOH gradient, TLC: R_f = 0.24, DCM:MeOH = 10:0.5). Yield: 111.01 mg (55 %). ^{1}H NMR ($CDCl_3$, 300.13 MHz) δ/ppm: 1.11–1.28 (m, 4H), 1.33–1.41 (m, 4H), 1.44 (d, 6H, J = 7 Hz), 2.92–3.03 (m, 2H), 3.18–3.29 (m, 2H), 4.65–4.75 (m, 2H), 6.82 (t, 2H, J = 5.5 Hz), 7.21 (d, 2H, J = 8 Hz), 7.24–7.34 (m, 22H), 7.74 (dt, 2H, J_1 = 7 Hz, J_2 = 1.5 Hz), 7.82 (dt, 2H, J_1 = 8 Hz, J_2 = 1 Hz). ^{13}C NMR ($CDCl_3$, 75.48 MHz) δ/ppm: 18.3 (β), 25.4 (c), 28.8 (b), 38.7 (a), 49.4 (α), 127.5 (4), 128.8 (d, $^3J_{CP}$ = 7 Hz, 3', 3''), 128.8 (d, $^3J_{CP}$ = 4 Hz, 5), 129.1 (4', 4''), 132.9 (d, $^2J_{CP}$ = 24.5 Hz, 2), 133.8 (d, $^2J_{CP}$ = 19.5 Hz, 2', 2''), 134.1 (d, $^3J_{CP}$ = 6.5 Hz, 3), 136.6 (d, $^1J_{CP}$ = 11 Hz, 1', 1''), 136.8 (d, $^2J_{CP}$ = 14 Hz, 6), 138.6 (d, $^1J_{CP}$ = 13 Hz, 1), 167.2 (7), 172.7 (A1). ESI-MS (m/z): 835.4 (M + H^+, 100 %). MALDI-HRMS (m/z): calc. 835.3536 ($C_{50}H_{52}N_4O_4P_2$ + H^+), found 835.3558.

7A. 3-(Diphenylphosphino)benzoic acid (123.6 mg, 0.40 mmol), HOBt (55.5 mg, 0.41 mmol), TBTU (124.8 mg, 0.39 mmol), DIPEA (0.145 mL, 0.88 mmol), **Boc-7A** (94.9 mg, 0.20 mmol), DCM (50 mL). Chromatography (DCM/MeOH gradient, TLC: R_f = 0.27, DCM:MeOH = 9.5:0.5). Yield: 84.4 mg (49 %). ^{1}H NMR ($CDCl_3$, 600.14 MHz) δ/ppm: 1.13 (s, 1H), 1.24–1.30 (m, 2H), 1.46 (d, 6H, J = 7 Hz), 2.87–2.92 (m, 2H), 3.23–3.28 (m, 2H), 4.75–4.80 (m, 2H), 6.96 (t, 2H, J = 5.5 Hz), 7.26–7.34 (m, 24H), 7.77 (dt, 2H, J_1 = 7.5 Hz, J_2 = 1.5 Hz), 7.85 (dt, 2H, J_1 = 8 Hz, J2 = 1.5 Hz). ^{13}C NMR ($CDCl_3$, 105.92 MHz) δ/ppm: 18.4 (β), 25.7 (c), 27.7 (d), 28.3 (b), 39.3 (a), 49.2 (α), 127.6 (4), 128.7 (5, overlaped with 3' peak), 128.8 (d, $^3J_{CP}$ = 7 Hz, 3', 3''), 129.1 (4', 4''), 133.1 (d, $^2J_{CP}$ = 26 Hz, 2), 133.9 (d, $^2J_{CP}$ = 20 Hz, 2'), 133.9 (d, $^2J_{CP}$ = 19 Hz, 2''), 134.1 (d, $^3J_{CP}$ = 8 Hz, 3), 136.6 (d, $^1J_{CP}$ = 11 Hz, 1', 1''), 136.8 (d, $^2J_{CP}$ = 14.5 Hz, 6), 138.5 (d, $^1J_{CP}$ = 13 Hz, 1), 167.2 (7), 172.8 (A1). ESI-MS (m/z): 849.4 (M + H^+, 100 %). MALDI-HRMS (m/z): calc. 849.3693 ($C_{51}H_{54}N_4O_4P_2$ + H^+), found 849.3696.

8A. 3-(Diphenylphosphino)benzoic acid (148.2 mg, 0.48 mmol), HOBt (71.0 mg, 0.53 mmol), TBTU (156.7 mg, 0.49 mmol), DIPEA (0.160 mL, 0.97 mmol), **Boc-8A** (107.4 mg, 0.22 mmol), DCM (50 mL). Chromatography (DCM/MeOH gradient, TLC: R_f = 0.15, EtOAc:Hexane = 7:3). Yield: 124.09 mg (59 %). ^{1}H NMR ($CDCl_3$, 300.13 MHz) δ/ppm: 1.14 (s, 8H), 1.29–1.37 (m, 4H), 1.44 (d, 6H, J = 7 Hz), 2.91–3.03 (m, 2H), 3.23–3.34 (m, 2H), 4.66–4.76 (m, 2H), 6.81 (t, 2H, J = 5.5 Hz), 7.07 (d, 2H, J = 8 Hz), 7.25–7.36 (m, 22H), 7.73–7.77 (m, 2H), 7.81 (d, 2H, J = 8 Hz). ^{13}C NMR ($CDCl_3$, 75.48 MHz) δ/ppm: 18.6 (β), 25.9 (c), 28.4 (d), 29.1 (b), 39.4 (a), 49.4

(α), 127.5 (4), 128.8 (d, $^{3}J_{CP}$ = 7 Hz, 3', 3''), 128.8 (d, $^{3}J_{CP}$ = 5 Hz, 5), 129.1 (4', 4''), 132.8 (d, $^{2}J_{CP}$ = 24.5 Hz, 2), 133.9 (d, $^{2}J_{CP}$ = 19.5 Hz, 2', 2''), 134.1 (d, $^{3}J_{CP}$ = 8 Hz, 3), 136.5 (d, $^{1}J_{CP}$ = 11 Hz, 1', 1''), 136.7 (d, $^{2}J_{CP}$ = 14 Hz, 6), 138.6 (d, $^{1}J_{CP}$ = 13.5 Hz, 1), 167.1 (7), 172.5 (A1). ESI-MS (m/z): 885.3 (M + Na^+, 14 %). MALDI-HRMS (m/z): calc. 863.3849 ($C_{52}H_{56}N_4O_4P_2$ + H^+), found 863.3835.

9A. 3-(Diphenylphosphino)benzoic acid (76.7 mg, 0.25 mmol), HOBt (39.2 mg, 0.29 mmol), TBTU (81.3 mg, 0.25 mmol), DIPEA (0.165 mL, 1.00 mmol), **Boc-9A** (60.2 mg, 0.11 mmol), DCM (50 mL). Chromatography (EtOAc/Hexane gradient, TLC: Rf = 0.49, EtOAc:Hexane = 7:3). Yield: 33.6 mg (33 %). ^{1}H NMR ($CDCl_3$, 300.14 MHz) δ/ppm: 1.49 (d, 6H, J = 7 Hz), 4.02 (dd, 2H, J_1 = 17.5 Hz, J_2 = 4.5 Hz), 4.30 (dd, 2H, J_1 = 17.5 Hz, J_2 = 6 Hz), 4.83–4.93 (m, 2H), 7.19–7.38 (m, 28H), 7.65 (pseudo-t, 2H, J = 5 Hz), 7.75 (dt, 2H, J_1 = 7.5 Hz, J_2 = 1 Hz), 7.86 (d, 2H, J_1 = 7.5 Hz, J_2 = 1 Hz). ^{13}C NMR ($CDCl_3$, 150.92 MHz) δ/ppm: 18.2 (β), 30.3 (a), 49.3 (α), 81.6 (b), 88.9 (c), 125.9 (d), 127.6 (4), 128.1 (f), 128.8 (d, $^{3}J_{CP}$ = 7 Hz, 3', 3''), 128.8 (5, under the 3' peak), 129.1 (4', 4''), 131.7 (e), 133.1 (d, $^{2}J_{CP}$ = 26 Hz, 2), 133.9 (d, $^{2}J_{CP}$ = 19 Hz, 2'), 133.9 (d, $^{2}J_{CP}$ = 19 Hz, 2''), 133.9 (d, $^{3}J_{CP}$ = 6 Hz, 3), 136.6 (d, $^{1}J_{CP}$ = 11 Hz, 1', 1''), 136.8 (d, $^{2}J_{CP}$ = 14 Hz, 6), 138.6 (d, $^{1}J_{CP}$ = 14 Hz, 1), 167.4 (7), 172.9 (A1). ^{31}P NMR ($CDCl_3$, 242.93 MHz) δ/ppm: –5.13. ESI-MS (m/z): 903.3 (M + H^+, 100 %). MALDI-HRMS (m/z): calc. 903.3223 ($C_{56}H_{48}N_4O_4P_2$ + H^+), found 903.3233.

9A$_p$. 4-(Diphenylphosphino)benzoic acid (145.4 mg, 0.48 mmol), HOBt (67.4 mg, 0.50 mmol), TBTU (151.3 mg, 0.47 mmol), DIPEA (0.235 mL, 1.42 mmol), **Boc-9A** (125.8 mg, 0.24 mmol), DCM (50 mL). Chromatography (EtOAc/Hexane gradient, TLC: R_f = 0.21, EtOAc:Hexane = 1:1). Yield: 105.3 mg (49 %). ^{1}H NMR ($CDCl_3$, 600.14 MHz) δ/ppm: 1.52 (d, 6H, J = 7 Hz), 4.04 (dd, 2H, J_1 = 17.5 Hz, J_2 = 4.5 Hz), 4.33 (dd, 2H, J_1 = 17.5 Hz, J_2 = 6.5 Hz), 4.90–4.95 (m, 2H), 7.18–7.22 (m, 6H), 7.25–7.27 (m, 8H), 7.29–7.33 (m, 14H), 7.49 (d, 2H, J = 8 Hz), 7.62 (dd, 2H, J_1 = 6 Hz, J_2 = 4.5 Hz), 7.72 (dd, 2H, J_1 = 8 Hz, J_2 = 1 Hz). ^{13}C NMR ($CDCl_3$, 75.48 MHz) δ/ppm: 18.2 (β), 30.3 (a), 49.2 (α), 81.6 (b), 88.9 (c), 125.9 (d), 127.3 (d, $^{3}J_{CP}$ = 6.5 Hz, 3,5), 128.2 (f), 128.8 (d, $^{3}J_{CP}$ = 7 Hz, 3', 3''), 129.2 (4', 4''), 131.7 (e), 133.5 (d, $^{2}J_{CP}$ = 19 Hz, 2,6), 133.7 (4), 134.0 (d, $^{2}J_{CP}$ = 20 Hz, 2', 2''), 136.4, 136.4 (d, $^{1}J_{CP}$ = 11 Hz, 1', 1''), 142.6 (d, $^{1}J_{CP}$ = 14 Hz, 1), 167.5 (7), 173.0 (A1). ESI-MS (m/z): 941.3 (M + K^+, 5 %). MALDI-HRMS (m/z): calc. 925.3043 ($C_{56}H_{48}N_4O_4P_2$ + H^+), found 925.3026.

9V. 3-(Diphenylphosphino)benzoic acid (114.1 mg, 0.37 mmol), HOBt (49.7 mg, 0.37 mmol), TBTU (119.6 mg, 0.37 mmol), DIPEA (0.130 mL, 0.79 mmol), **Boc-9V** (110.0 mg, 0.19 mmol), DCM (50 mL). Chromatography (EtOAc/Hexane gradient, TLC: R_f = 0.41, EtOAc:Hexane = 1:1). Yield: 84.8 mg (47 %). ^{1}H NMR ($CDCl_3$, 300.14 MHz) δ/ppm: 0.97 (d, 6H, J = 6.5 Hz), 0.98 (d, 6H, J = 6.5 Hz), 2.15–2.27 (m, 2H), 3.95 (dd, 2H, J_1 = 17.5 Hz, J_2 = 4.5 Hz), 4.35 (dd, 2H, J_1 = 17.5 Hz, J_2 = 6.5 Hz), 4.60 (dd, 2H, J_1 = J_2 = 8.5 Hz), 7.17–7.35 (m, 30H), 7.71–7.78 (m, 6H). ^{13}C NMR ($CDCl_3$, 75.48 MHz) δ/ppm: 19.0, 19.5 (γ), 30.0 (a), 31.0 (β), 59.5 (α), 81.3 (b), 89.0 (c), 125.8 (d), 127.6 (4), 128.0 (f), 128.7 (5, under the 3' peak), 128.7 (d, $^{3}J_{CP}$ = 7 Hz, 3', 3''), 129.1 (4', 4''), 131.8 (e), 132.9 (d, $^{2}J_{CP}$ = 24 Hz, 2), 133.9 (d, $^{2}J_{CP}$ = 20 Hz, 2'), 133.9 (d, $^{2}J_{CP}$ = 20 Hz, 2''), 134.2 (d, $^{3}J_{CP}$ = 7 Hz, 3), 136.6 (d, $^{1}J_{CP}$ = 10.5 Hz, 1'), 136.6 (d, $^{1}J_{CP}$ = 10.5 Hz, 1''), 136.8 (d, $^{2}J_{CP}$ = 16 Hz, 6), 138.5 (d, $^{1}J_{CP}$ = 13 Hz, 1), 167.6 (7), 172.0 (V1). ESI-MS (m/z): 981.4 (M + Na^+, 22 %). MALDI-HRMS (m/z): calc. 959.3849 ($C_{60}H_{56}N_4O_4P_2$ + H^+), found 959.3851.

9L. 3-(Diphenylphosphino)benzoic acid (90.3 mg, 0.30 mmol), HOBt (40.4 mg, 0.30 mmol), TBTU (93.0 mg, 0.29 mmol), DIPEA (0.100 mL, 0.61 mmol), **Boc-9L** (83.7 mg, 0.14 mmol), DCM (50 mL). Chromatography (EtOAc/Hexane gradient, TLC: R_f = 0.28, EtOAc:Hexane = 1:1). Yield: 51.1 mg (38 %). ^{1}H NMR ($CDCl_3$, 600.14 MHz) δ/ppm: 0.88 (d, 6H, J = 6 Hz), 0.90 (d, 6H, J = 6 Hz), 1.62–1.76 (m, 6H), 3.85 (dd, 2H, J_1 = 17.5 Hz, J_2 = 4.5 Hz), 4.27 (dd, 2H, J_1 = 17.5 Hz, J_2 = 6.5 Hz), 4.83–4.87 (m, 2H), 7.11 (d, 2H, J = 8 Hz), 7.17–7.19 (m, 2H), 7.22 (t, 2H, J = 7.5 Hz), 7.25–7.34 (m, 20H), 7.69 (d, 2H, J = 8 Hz), 7.76 (d, 2H, J = 8 Hz), 7.79 (pseudo-t, 2H, J = 5.5 Hz). ^{13}C NMR ($CDCl_3$, 75.48 MHz) δ/ppm: 22.2, 23.1 (δ), 25.0 (γ), 30.1 (a), 41.0 (β), 52.3 (α), 81.3 (b), 89.0 (c), 125.6 (d), 127.5 (4), 127.9 (f), 128.7 (d, $^3J_{CP}$ = 7 Hz, 3', 3''), 128.8 (5, under the 3' peak), 129.1, 129.1 (4', 4''), 131.8 (e), 132.8 (d, $^2J_{CP}$ = 23 Hz, 2), 133.9 (d, $^2J_{CP}$ = 19.5 Hz, 2'), 133.9 (d, $^2J_{CP}$ = 19.5 Hz, 2''), 134.0 (d, $^3J_{CP}$ = 7 Hz, 3), 136.6 (d, $^1J_{CP}$ = 11 Hz, 1'), 136.6 (d, $^1J_{CP}$ = 11 Hz, 1''), 136.8 (d, $^2J_{CP}$ = 16.5 Hz, 6), 138.4 (d, $^1J_{CP}$ = 13 Hz, 1), 167.5 (7), 172.9 (L1). ESI-MS (m/z): 1009.4 (M + Na^+, 29 %). MALDI-HRMS (m/z): calc. 987.4162 ($C_{62}H_{60}N_4O_4P_2 + H^+$), found 987.4164.

9L$_p$. 4-(Diphenylphosphino)benzoic acid (80.4 mg, 0.26 mmol), HOBt (37.5 mg, 0.28 mmol), TBTU (85.4 mg, 0.27 mmol), DIPEA (0.090 mL, 0.55 mmol), **Boc-9L** (75.9 mg, 0.12 mmol), DCM (50 mL). Chromatography (EtOAc/Hexane gradient, TLC: R_f = 0.33, EtOAc:Hexane = 1:1). Yield: 36.7 mg (30 %). ^{1}H NMR ($CDCl_3$, 600.14 MHz) δ/ppm: 0.93 (d, 6H, J = 6 Hz), 0.95 (d, 6H, J = 6 Hz), 1.52–1.56 (m, 2H), 1.71–1.78 (m, 4H), 3.92 (dd, 2H, J_1 = 17.5 Hz, J_2 = 4 Hz), 4.30 (dd, 2H, J_1 = 17.5 Hz, J_2 = 7 Hz), 4.86–4.90 (m, 2H), 7.25–7.20 (m, 8H), 7.26–7.35 (m, 26H), 7.66–7.67 (m, 6H). ^{13}C NMR (DMSO-d_6, 75.48 MHz) δ/ppm: 21.2, 23.0 (δ), 24.4 (γ), 28.9 (a), 40.3 (β), 51.7 (α), 80.0 (b), 90.9 (c), 124.8 (d), 127.7 (d, $^3J_{CP}$ = 7 Hz, 3, 5), 128.4 (f), 128.8 (d, $^3J_{CP}$ = 7 Hz, 3', 3''), 129.2 (4', 4''), 131.8 (e), 132.7 (d, $^2J_{CP}$ = 19 Hz, 2), 133.3 (d, $^2J_{CP}$ = 20 Hz, 2', 2''), 134.3 (4), 136.0 (d, $^1J_{CP}$ = 11 Hz, 1'), 136.1 (d, $^1J_{CP}$ = 11 Hz, 1''), 140.7 (d, $^1J_{CP}$ = 13 Hz, 1), 166.0 (7), 172.1 (L1). ESI-MS (m/z): 1009.4 (M + Na^+, 18 %). MALDI-HRMS (m/z): calc. 1009.3982 ($C_{62}H_{60}N_4O_4P_2 + Na^+$), found 1009.3978.

9F. 3-(Diphenylphosphino)benzoic acid (98.6 mg, 0.32 mmol), HOBt (47.5 mg, 0.35 mmol), TBTU (103.7 mg, 0.32 mmol), DIPEA (0.200 mL, 1.21 mmol), **Boc-9F** (101.6 mg, 0.15 mmol), DCM (50 mL). Chromatography (EtOAc/Hexane gradient, TLC: R_f = 0.47, EtOAc:Hexane = 1:1). Yield: 69.7 mg (44 %). ^{1}H NMR ($CDCl_3$, 600.14 MHz) δ/ppm: 3.11 (dd, 2H, J_1 = 14 Hz, J_2 = 8 Hz), 3.20 (dd, 2H, J_1 = 14 Hz, J_2 = 7 Hz), 3.90 (dd, 2H, J_1 = 17.5 Hz, J_2 = 4.5 Hz), 4.20 (dd, 2H, J_1 = 17.5 Hz, J_2 = 6 Hz), 5.02–5.06 (m, 2H), 7.09–7.33 (m, 40H), 7.49 (t, 2H, J = 5.5 Hz), 7.61 (d, 2H, J = 7.5 Hz), 7.72 (d, 2H, J = 8 Hz). ^{13}C NMR ($CDCl_3$, 75.48 MHz) δ/ppm: 30.1 (a), 38.5 (β), 55.1 (α), 81.5 (b), 88.8 (c), 125.7 (d), 127.0 (ζ), 127.6 (4), 128.1 (f), 128.6 (δ), 128.7 (5, under the 3' peak), 128.8 (d, $^3J_{CP}$ = 7 Hz, 3', 3''), 129.1 (4', 4''), 129.4 (ε), 131.8 (e), 132.8 (d, $^2J_{CP}$ = 24 Hz, 2), 133.9 (d, $^2J_{CP}$ = 20 Hz, 2', 2''), 133.9 (d, $^3J_{CP}$ = 7.5 Hz, 3), 136.6 (d, $^1J_{CP}$ = 11 Hz, 1'), 136.6 (d, $^1J_{CP}$ = 11 Hz, 1''), 136.8 (γ), 136.8 (d, $^2J_{CP}$ = 15.5 Hz, 6), 138.5 (d, $^1J_{CP}$ = 13.5 Hz, 1), 167.5 (7), 171.7 (F1). ESI-MS (m/z): 1055.2 (M + H^+, 39 %). MALDI-HRMS (m/z): calc. 1055.3849 ($C_{68}H_{56}N_4O_4P_2 + H^+$), found 1055.3872.

10A. 3-(Diphenylphosphino)benzoic acid (66.4 mg, 0.22 mmol), HOBt (29.4 mg, 0.22 mmol), TBTU (69.6 mg, 0.22 mmol), DIPEA (0.145 mL, 0.88 mmol), **Boc-10A** (100.0 mg, 0.19 mmol), DCM (50 mL). Chromatography (EtOAc/Hexane gradient, TLC: R_f = 0.21, EtOAc:Hexane = 7:3). Yield: 26.6 mg (27 %). ^{1}H NMR (DMSO-d_6, 300.13 MHz) δ/ppm: 1.31 (d, 6H, J = 7 Hz), 1.57–1.67 (m, 4H), 2.52–2.56 (m, 4H, solvent overlaped), 3.03–3.15 (m, 4H), 4.36–4.46 (m, 2H),

7.05–7.13 (m, 4H), 7.22–7.31 (m, 10H), 7.38–7.42 (m, 11H), 7.45–7.51 (m, 3H), 7.89–7.95 (m, 6H), 8.54 (d, 2H, J_1 = 7.5 Hz, J_2 = 1 Hz). ^{13}C NMR (DMSO-d_6, 75.48 MHz) δ/ppm: 18.0 (β), 29.1 (c), 30.7 (b), 38.4 (a), 49.1 (α), 125.8 (f), 128.0 (4), 128.6 (d, $^3J_{CP}$ = 6 Hz, 5), 128.8 (d, $^3J_{CP}$ = 7 Hz, 3', 3''), 128.9 (e), 129.1, (4', 4''), 132.7 (d, $^2J_{CP}$ = 26 Hz, 2), 133.2 (d, $^2J_{CP}$ = 20 Hz, 2'), 133.2 (d, $^2J_{CP}$ = 20 Hz, 2''), 134.3 (d, $^3J_{CP}$ = 8 Hz, 3), 135.6 (d, $^2J_{CP}$ = 14 Hz, 6), 136.2 (d, $^1J_{CP}$ = 11 Hz, 1'), 136.2 (d, $^1J_{CP}$ = 11 Hz, 1''), 137.0 (d, $^1J_{CP}$ = 12.5 Hz, 1), 139.4 (d), 165.5 (7), 172.1 (A1). ESI-MS (m/z): 911.4 (M + H^+, 34 %). MALDI-HRMS (m/z): calc. 911.3849 ($C_{56}H_{56}N_4O_4P_2$ + H^+), found 911.3828.

10A$_p$. 4-(Diphenylphosphino)benzoic acid (66.0 mg, 0.22 mmol), HOBt (67.4 mg, 0.50 mmol), TBTU (70.0 mg, 0.22 mmol), DIPEA (0.145 mL, 0.88 mmol), **Boc-10A** (100.0 mg, 0.19 mmol), DCM (50 mL). Chromatography (EtOAc/Hexane gradient, TLC: R_f = 0.24, EtOAc:Hexane = 7:1). Yield: 58.2 mg (59 %). ^{1}H NMR (DMSO-d_6, 300.13 MHz) δ/ppm: 1.32 (d, 6H, J = 7 Hz), 1.59–1.69 (m, 4H), 2.52–2.57 (m, 4H), 3.07–3.15 (m, 4H), 4.39–4.48 (m, 2H), 7.05–7.13 (m, 4H), 7.23–7.31 (m, 12H), 7.39–7.43 (m, 12H), 7.88 (dd, 4H, J_1 = 8 Hz, J_2 = 1 Hz), 7.94 (pseudo-t, 2H, J = 5.5 Hz), 8.46 (d, 2H, J = 7.5 Hz). ^{13}C NMR (DMSO-d_6, 75.48 MHz) δ/ppm: 18.0 (β), 29.2 (c), 30.7 (b), 38.4 (a), 49.1 (α), 125.8 (f), 127.7 (d, $^3J_{CP}$ = 6.5 Hz, 3,5), 128.8 (d, $^3J_{CP}$ = 7 Hz, 3', 3''), 128.9 (e), 129.2 (4', 4''), 132.7 (d, $^2J_{CP}$ = 19 Hz, 2), 133.3 (d, $^2J_{CP}$ = 19.5 Hz, 2', 2''), 133.4 (4), 136.1 (d, $^1J_{CP}$ = 11 Hz, 1', 1''), 139.4 (d), 140.65 (d, $^1J_{CP}$ = 13.5 Hz, 1), 165.6 (7), 172.1 (A1). ESI-MS (m/z): 925.4 (M + H^+, 32 %). MALDI-HRMS (m/z): calc. 925.3043 ($C_{56}H_{48}N_4O_4P_2$ + Na^+), found 925.3026.

10L. 3-(Diphenylphosphino)benzoic acid (109.2 mg, 0.36 mmol), HOBt (50.7 mg, 0.38 mmol), TBTU (113.4 mg, 0.35 mmol), DIPEA (0.120 mL, 0.73 mmol), **Boc-10L** (105.0 mg, 0.17 mmol), DCM (50 mL). Chromatography (EtOAc/Hexane gradient, TLC: R_f = 0.47, EtOAc:Hexane = 1:1). Yield: 57.8 mg (33 %). ^{1}H NMR ($CDCl_3$, 600.14 MHz) δ/ppm: 0.89 (d, 6H, J = 6.5 Hz), 0.90 (d, 6H, J = 6.5 Hz), 1.42–1.57 (m, 4H), 1.61–1.70 (m, 6H), 2.28–2.33 (m, 2H), 2.42–2.47 (m, 2H), 2.66–2.70 (m, 2H), 3.48–3.54 (m, 2H), 4.86–4.90 (m, 2H), 6.86 (d, 2H, J = 9 Hz), 6.97–7.00 (m, 2H), 7.04–7.07 (m, 2H), 7.25–7.34 (m, 22H), 7.39–7.41 (m, 2H), 7.67–7.69 (m, 2H), 7.71–7.73 (m, 2H), 7.97–7.98 (m, 2H). ^{13}C NMR ($CDCl_3$, 75.48 MHz) δ/ppm: 22.4, 22.9 (δ), 25.0 (γ), 29.5 (c), 31.4 (b), 39.1 (a), 41.4 (β), 52.6 (α), 126.1 (f), 127.2 (4), 128.8 (d, $^3J_{CP}$ = 7 Hz, 3', 3''), 128.8 (d, $^2J_{CP}$ = 6 Hz, 5), 129.2, 129.2 (4', 4''), 129.3 (e), 132.6 (d, $^2J_{CP}$ = 21 Hz, 2), 133.8 (d, $^2J_{CP}$ = 20 Hz, 2'), 134.0 (d, $^2J_{CP}$ = 20 Hz, 2''), ≈ 133.9 (3, not observable because overlap), 136.5 (d, $^1J_{CP}$ = 11 Hz, 1'), 136.5 (d, $^1J_{CP}$ = 11 Hz, 1''), 136.9 (d, $^2J_{CP}$ = 18 Hz, 6), 138.7 (d, $^1J_{CP}$ = 13.5 Hz, 1), 139.8 (d), 167.3 (7), 172.8 (A1). ^{31}P NMR ($CDCl_3$, 242.93 MHz) δ/ppm: –4.96. ESI-MS (m/z): 1033.5 (M + K^+, 23 %). MALDI-HRMS (m/z): calc. 1033.4374 ($C_{62}H_{68}N_4O_4P_2$ + K^+), found 1033.4388.

10L$_p$. 4-(Diphenylphosphino)benzoic acid (110.1 mg, 0.36 mmol), HOBt (49.8 mg, 0.37 mmol), TBTU (114.2 mg, 0.36 mmol), DIPEA (0.120 mL, 0.73 mmol), **Boc-10L** (105.0 mg, 0.17 mmol), DCM (50 mL). Chromatography (EtOAc/Hexane gradient, TLC: R_f = 0.47, EtOAc:Hexane = 1:1). Yield: 63.5 mg (36 %). ^{1}H NMR ($CDCl_3$, 600.14 MHz) δ/ppm: 0.94 (d, 6H, J = 6 Hz), 0.95 (d, 6H, J = 6.5 Hz), 1.49–1.60 (m, 4H), 1.67–1.77 (m, 6H), 2.35–2.46 (m, 4H), 2.85–2.90 (m, 2H), 3.48–3.54 (m, 2H), 4.90–4.93 (m, 2H), 6.98–7.00 (m, 2H), 7.03–7.05 (m, 2H), 7.20 (d, 2H, J = 9 Hz), 7.23–7.35 (m, 24H), 7.68 (dd, 2H, J_1 = 8.5 Hz, J_2 = 1 Hz), 7.84 (dd, 2H, J_1 = 8 Hz, J_2 = 4 Hz). ^{13}C NMR ($CDCl_3$, 75.48 MHz) δ/ppm: 22.4, 23.0 (δ), 25.1 (γ),29.7 (c), 31.1 (b), 39.3 (a), 41.3 (β), 52.5 (α), 81.6 (b), 88.9 (c), 126.2 (f), 127.2 (d, $^3J_{CP}$ = 6.5 Hz, 3,5), 128.8 (d, $^3J_{CP}$ = 7

Hz, 3', 3''), 129.1 (e), 129.2 (4', 4''), 133.5 (d, $^2J_{CP}$ = 19 Hz, 2), 133.8 (4), 134.0 (d, $^2J_{CP}$ = 20 Hz, 2', 2''), 136.4 (d, $^1J_{CP}$ = 11 Hz, 1', 1''), 139.6 (d), 142.7 (d, $^1J_{CP}$ = 14 Hz, 1), 167.5 (7), 172.9 (A1). ESI-MS (m/z): 1033.4 ($M + K^+$, 10 %). MALDI-HRMS (m/z): calc. 1017.4608 ($C_{62}H_{68}N_4O_4P_2 + Na^+$), found 1017.4615.

Precatalytic Rh(I) complexes.

NMR measurements. $[Rh(COD)(CH_3CN)_2]BF_4$ (1 mg, 2.6 μmol, 1 equiv.) and ligand (2 equiv.) were each dissolved in of $CDCl_3$ (300 μL). Rhodium solution was added to the ligand solution and NMR spectra were recorded shortly thereafter.

CD measurements. VIS region (c = 0.15–0.44 mmol dm^{-3}): $[Rh(COD)(CH_3CN)_2]BF_4$ (1 equiv.) and the ligand (2 equiv.) were each dissolved in 2 mL of distilled, degassed CH_2Cl_2. This was then mixed, diluted to 5.0 mL. UV region (c = 0.01–0.03 mmol dm^{-3}): 300 μL of the solution for VIS measurements was diluted to 5.0 mL.

Catalysis.

Catalytic Hydrogenation of methyl 2-acetamidoacrylate (**S1**). (a) Catalysis at room temperature: An oven-dried, two-necked, round bottomed flask (10 mL) under nitrogen was charged with the ligand (6.6 μmol, 2.2 mol-%) dissolved in CH_2Cl_2 (3 mL; distilled, degassed in an ultrasonic bath for 15 min), followed by $[Rh(COD)(CH_3CN)_2]BF_4$ (1.25 mg, 3 μmol, 1 mol-%) dissolved in CH_2Cl_2 (2 mL). Several experiments were performed in diluted CH_2Cl_2 solution (total volume 50 mL instead of 5 mL) or in methanol (total volume 5 mL). The flask was then flushed with hydrogen, and **S1** (45 mg, 0.3 mmol) was added in one portion and vigorously stirred with a magnetic stirrer. After 2 h, 0.5 mL of the solution was eluted through silica (150 mg) with ethyl acetate (5 mL), and the enantiomeric excess (ee) was determined by chiral fused silica capillary column [Beta Dex 225; isocratic 140 or 150 °C; 100 kPa head column pressure; eluting order: substrate, (*R*) product, (*S*) product]. (b) Catalysis at Low Temperature: According to the procedure for reactions at room temperature before substrate addition, the reaction flask was placed in a thermo-container filled with technical ethanol (or 2-propanol), cooled by a cryostat device to –5 °C, and the mixture was stirred vigorously overnight.

Catalytic Hydrogenation of methyl (Z)-α-acetamidocinnamate (**S2**). (a) Catalysis at atmospheric pressure: The procedure described for **S1** was used with ligand (13.2 μmol, 2.2 mol-%), $[Rh(COD)(CH_3CN)_2]BF_4$ (2.50 mg, 6 μmol, 1 mol-%) and **S2** (70 mg, 0.3 mmol). Chiral fused silica capillary column [L-chirasil-Val; conditions: 22 min at 170 °C; 40 °C min^{-1} to 190 °C, 60 kPa head column pressure; t_R = 18.30 (*R*), 18.75 (*S*), 32.39 (substrate) min]. (b) Catalysis at High Pressure: In an Eppendorf vial, Rh precursor and the ligand were dissolved in CH_2Cl_2 (0.5 mL each) and mixed. The yellow solution was added to a 10 mL beaker containing the substrate and CH_2Cl_2 (4 mL). This was tightly sealed in an autoclave and purged three times with H_2 (13 bar) and finally stirred at 13 bar for 2 h. The product was analyzed as detailed above.

Associated content.

Supporting Information. Synthetic procedures for the precursors **Boc-2** – **Boc-10**, catalytic asymmetric hydrogenation using *para*-substituted ligands, NMR and CD spectra, GC chromatograms, visualized calculated structures of various conformers and stereochemical analysis. Cartesian coordinates for all computed molecules are collected in a single separate text file readable by the program Mercury (version 3.3 or later)[33] for visualization and analysis. This material is available free of charge *via* the Internet at http://pubs.acs.org

Author information.

Corresponding Author. E-mail for S.I.K.: Srecko.Kirin@irb.hr

Notes. The authors declare no competing financial interests.

Acknowledgments.

These materials are based on work financed by the Unity Through Knowledge Fund (UKF, 36/08), the Croatian Science Foundation (HrZZ, 02.04/23) and the Ministry of Science, Education and Sports (MSES, 098-0982904-2946, 098-0982933-2908 and 098-0982933-2936). We thank COST Action CM1105 for financial support.

References.

(1) Liskamp, R. M. J.; Rijkers, D. T. S.; Kruijtzer, J. A. W.; Kemmink, J. *ChemBioChem* **2011**, *12*, 1626–1653.

(2) (a) Vasudev, P. G.; Chatterjee, S.; Shamala, N.; Balaram. P. *Chem. Rev.* **2011**, *111*, 657–687; (b)Vagner, J.; Qu, H.; Hruby, V. J. *Curr. Opin. Chem. Biol.* **2008**, *12*, 292–296.

(3) Kahn, M.; Eguchi, M.; In: *Synthesis of peptides and peptidomimetics*. 4th Ed.; Goodman, M.; Felix, A. F.; Moroder, L.; Toniolo, C.; Eds.; Georg Thieme Verlag: Stuttgart, Germany, **2004**; Vol. E22c, pp. 695–758.

(4) Chouhan, G.; James, K. *Org. Lett.* **2013**, *15*, 1206–1209.

(5) Hack, V.; Reuter, C.; Opitz, R.; Schmieder, P.; Beyermann, M.; Neudorfl, J.-M.; Kuhne, R.; Schmalz, H.-G. *Angew. Chem. Int. Ed.* **2013**, *52*, 1–6.

(6) Garland, S. L.; Dean, P. M. *J. Comput. - Aided Mol. Des.* **1999**, *13*, 469–483.

(7) Gredičak, M.; Bregović, N.; Carić, D.; Jerić, I. *J. Inorg. Biochem.* **2012**, *116*, 45–52.

(8) (a) Kokan, Z.; Kirin, S. I. *Eur. J. Org. Chem.* **2013**, 8154–8161; (b) Kokan, Z.; Kirin S. I., *RSC Adv.* **2012**, *2*, 5729–5737.

(9) Other catalysts with prochiral metal coordination sphere: (a) Kanda, K.; Oshima, S.; Shizuno, T.; Hamanaka, R.; Fukai, M.; Shibata, T. *Heterocycles* **2014**, *88*, 1355–1370; (b) Raynal, M.; Portier, F.; van Leeuwen, P. W. N. M.; Bouteiller, L. *J. Am. Chem. Soc.* **2013**, *135*, 17687−17690; (c) van Leeuwen, P. W. N. M.; Rivillo, D.; Raynal, M.; Freixa, Z. *J. Am. Chem. Soc.* **2011**, *133*, 18562–18565; (d) Laungani, A. C.; Breit, B. *Chem. Commun.* **2008**, 844–846.

(10) Other hydrogenation catalysts: (a) Wang, X.-B.; Goto, M.; Han, L.-B. *Chem. Eur. J.* **2014**, *20*, 3631–3635; (b) Thacker, N. C.; Moteki, S. A.; Takacs, J. M. *ACS Catal.* **2012**, *2*, 2743–2752; (c) Pignataro, L.; Boghi, M.; Civera, M.; Carboni, S.; Piarulli, U.; Gennari, C. *Chem. Eur.*

J. **2012**, *18*, 1383–1400; (d) Dydio, P.; Rubay, C.; Gadzikwa, T.; Lutz, M.; Reek, J. N. H. *J. Am. Chem. Soc.* **2011**, *133*, 17176–17179; (e) Sambasivan, R.; Ball, Z. T. *J. Am. Chem. Soc.* **2010**, *132*, 9289–9291; (f) Gilbertson, S. R.; Collibee, S. E.; Agarkov, A. *J. Am. Chem. Soc.* **2000**, *122*, 6522–6523.

(11) Recent reviews on bioinspired catalysis: (a) Raynal, M.; Ballester, P.; Vidal-Ferran, A.; van Leeuwen, P. W. N. M. *Chem. Soc. Rev.* **2014**, 43, 1660–1733; (b) Lewis, J. C. *ACS Catal.* **2013**, *3*, 2954−2975; (c) Dong, Z.; Luo, Q.; Liu, J. *Chem. Soc. Rev.* **2012**, *41*, 7890–7908; (d) Deuss, P. J.; Heeten, R.; Laan, W.; Kamer, P. C. J. *Chem. Eur. J.* **2011**, *17*, 4680–4698.

(12) (a) Gridnev, I. D.; Imamoto, T. *Acc. Chem. Res.* **2004**, *37*, 633–644; (b) Tangand, W.; Zhang, X. *Chem. Rev.* **2003**, *103*, 3029–3069; (c) Landis, C. R.; Halpern, J. *J. Am. Chem. Soc.* **1987**, *109*, 1746–1754; (d) Imamoto, T.; Tamura, K.; Zhang, Z.; Horiuchi, Y.; Masashi Sugiya, M.; Kazuhiro Yoshida, K.; Akira Yanagisawa, A.; Gridnev, I. D. *J. Am. Chem. Soc.* **2012**, *134*, 1754−1769.

(13) Kirin, S. I.; Kraatz, H.-B.; Metzler-Nolte, N. *Chem. Soc. Rev.* **2006**, *35*, 348–354.

(14) (a) Jarvis, A. G.; Sehnal, P. E.; Bajwa, S. E.; Whitwood, A. C.; Zhang, X.; Cheung, M. S.; Lin, Z.; Fairlamb, I. J. S. *Chem. Eur. J.* **2013**, *19*, 6034–6043; (b) Dydio, P.; Dzik, W. I.; Lutz, M.; de Bruin, B.; Reek, J. N. H. *Angew. Chem. Int. Ed.* **2011**, *50*, 396–400; (c) van Leeuwen, P. W. N. M.; Kamer, P. C. J.; Reek, J. N. H.; Dierkes, P. *Chem. Rev.* **2000**, *100*, 2741–2769.

(15) Herd, O.; Heβler, A.; Hingst, M.; Tepper, M.; Stelzer, O. *J. Organomet. Chem.* **1996**, *522*, 69–76.

(16) Grdičak, M.; Kolonić, A.; Jerić, I. *Amino Acids* **2008**, *35*, 185–194.

(17) (a) Martinez, C. R.; Iverson, B. L. *Chem. Sci.* **2012**, *3*, 2191–2201; (b) Lee, E. C.; Kim, D.; Jurecka, P.; Tarakeshwar, P.; Hobza, P.; Kim, K. S. *J. Phys. Chem. A* **2007**, *111,* 3446–3457; (c) Meyer, E. A.; Castellano, R. K.; Diederich, F. *Angew. Chem. Int. Ed.* **2003**, *42*, 1210–1250; (d) Janiak, C. *J. Chem. Soc., Dalton Trans.* **2000**, 3885–3896.

(18) For CD spectra of $[Rh(COD)(PPh_3)_2]$ derivatives see ref. 8 and: Yu, J.; Rajan Babu, T. V.; Parquette, J. R. *J. Am. Chem. Soc.* **2008**, *130*, 7845–7847.

(19) For CD spectra of ferrocene peptides $[Fe(C_5H_4CO\text{-}Aa_n\text{-}R)_2]$ (Herrick-conformation) see ref. 12 and: Kirin, S. I.; Schatzschneider, U.; Koster, S. D.; Siebler D.; Metzler-Nolte, N. *Inorg. Chim. Acta* **2009**, *362*, 894–906.

(20) The correlation between the CD spectra and molecular conformation is known to be rather difficult, see for example: Brkljača, Z.; Čondić-Jurkić, K.; Smith, A.-S.; Smith, D. M. *J. Chem. Theory Comput.* **2012**, *8*, 1694–1705 and references cited therein.

(21) (a) Kretschmer, R.; Schlangen, M.; Schwarz, H. *Dalton Trans.* **2013**, *42*, 4153–4162; (b) Armelin, M.; Schlangen, M.; Schwarz, H. *Chem Eur. J.* **2008**, *14*, 5229–5236.

(22) Zhao, Y.; Truhlar, D. G. *Theor. Chem. Acc.* **2008**, *120*, 215–241.

(23) (a) Leseurre, L.; d' Herouville, F. L. B.; Püntener, K.; Scalone, M.; Genet, J.-P.; Michelet, V. *Org. Lett.* **2011**, *13*, 3250–3253; (b) Preetz, A.; Drexler, H.-J.; Schulz, S.; Heller, D. *Tetrahedron: Asymmetry* **2010**, *21*, 1226–1231; (c) Kaganovsky, L.; Cho, K.-B.; Gelman, D. *Organometallics* **2008**, *27*, 5139–5145; (d) Punniyamurthy, T.; Mayr, M.; Dorofeev, A. S.; Bataille, C. J. R.; Gosiewska, S.; Nguyen, B.; Cowley, A. R.; Brown, J. M. *Chem.Commun.* **2008**, 5092–5094; (e) Albers, J.; Dinjus, E.; Pitter, S.; Walter, O. *J. Mol. Catal. A: Chem.* **2004**, *219*, 41–46; (f) Nishihara, Y.; Nara, K.; Nishide, Y.; Osakada, K. *Dalton Trans. 2004*, 1366–1375; (g) Zhang, X.; Mashima, K.; Koyano, K.; Sayo, N.; Kumobayashi, H.; Akutagawa, S.; Takaya, H. *J. Chem. Soc., Perkin Trans. 1* **1994**, 2309–2322.

(24) Bernstein, J.; Davis, R. E.; Shimoni, L.; Chang, H.-L. *Angew. Chem. Int. Ed. Engl.* **1995**, *34*, 1555–1573.

(25) Interestingly, in all known examples of triphenylphosphanes,[9d] ferrocenes,[12,26] and benzene 1,3,5-tricarboxylic acids[27] L-amino acids always induce a *P*-helix of the central aromatic unit.

(26) For secondary structures in ferrocene amino acid bioconjugates see: (a) Barišić, L.; Čakić, M.; Mahmoud, K. A.; Liu, Y.-N.; Kraatz, H.-B.; Pritzkow, H.; Kirin, S. I.; Metzler-Nolte, N.; Rapić, V. *Chem. Eur. J.* **2006**, *12*, 4965–4980; (b) Heinze, K.; Beckmann, M. *Eur. J. Inorg. Chem.* **2005**, 3450–3457; (c) Moriuchi, T.; Nomoto, A.; Yoshida, K.; Ogawa, A.; Hirao, T. *J. Am. Chem. Soc.* **2001**, *123*, 68–75; (d) Herrick, R. S.; Jarret, R. M.; Curran, T. P.; Dragoli, D. R.; Flaherty, M. B.; Lindyberg, S. E.; Slate, R. A.; Thornton, L. C. *Tetrahedron Lett.* **1996**, *37*, 5289–5292.

(27) For secondary structures in amino acid bioconjugates of benzene 1,3,5-tricarboxylic acid see: (a) Sun, R.; Wang, S.; Xing, H.; Bai, J.; Li, Y.; Pan, Y.; You, X. *Inorg. Chem.* **2007**, *46*, 8451–8453; (b) Bose, P. P.; Drew, M. G. B.; Das, A. K.; Banerjee, A. *Chem. Commun.* **2006**, 3196–3198.

(28) Gaussian 09, Revision A.02, Frisch, M. J.; Trucks, G. W.; Schlegel, H. B.; Scuseria, G. E.; Robb, M. A.; Cheeseman, J. R.; Scalmani, G.; Barone, V.; Mennucci, B.; Petersson, G. A.; Nakatsuji, H.; Caricato, M.; Li, X.; Hratchian, H. P.; Izmaylov, A. F.; Bloino, J.; Zheng, G.; Sonnenberg, J. L.; Hada, M.; Ehara, M.; Toyota, K.; Fukuda, R.; Hasegawa, J.; Ishida, M.; Nakajima, T.; Honda, Y.; Kitao, O.; Nakai, H.; Vreven, T.; Montgomery, J. A., Jr.; Peralta, J. E.; Ogliaro, F.; Bearpark, M.; Heyd, J. J.; Brothers, E.; Kudin, K. N.; Staroverov, V. N.; Kobayashi, R.; Normand, J.; Raghavachari, K.; Rendell, A.; Burant, J. C.; Iyengar, S. S.; Tomasi, J.; Cossi, M.; Rega, N.; Millam, N. J.; Klene, M.; Knox, J. E.; Cross, J. B.; Bakken, V.; Adamo, C.; Jaramillo, J.; Gomperts, R.; Stratmann, R. E.; Yazyev, O.; Austin, A. J.; Cammi, R.; Pomelli, C.; Ochterski, J. W.; Martin, R. L.; Morokuma, K.; Zakrzewski, V. G.; Voth, G. A.; Salvador, P.; Dannenberg, J. J.; Dapprich, S.; Daniels, A. D.; Farkas, Ö.; Foresman, J. B.; Ortiz, J. V.; Cioslowski, J.; Fox, D. J. Gaussian, Inc., Wallingford CT, 2009.

(29) (a) Becke, A. D. *J. Chem. Phys.* **1993**, *98*, 5648–5652; (b) Lee, C.; Yang, W.; Parr, R. G. *Phys. Rev. B* **1988**, *37*, 785–789; (c) Miehlich, B.; Savin, A.; Stoll, H.; Preuss, H. *Chem. Phys. Lett.* **1989**, *157*, 200–206.

(30) (a) Schäfer, A.; Horn, H.; Ahlrichs, R. *J. Chem. Phys.* **1992**, *97*, 2571–2577; (b) Schäfer, A.; Huber, C.; Ahlrichs, R. *J. Chem. Phys.* **1994**, *100*, 5829–5835.

(31) (a) Hay, P. J.; Wadt, W. R. *J. Chem. Phys.* **1985**, *82*, 270–283; (b) Hay, P. J.; Wadt, W. R. *J. Chem. Phys.* **1985**, *82*, 299–310; (c) Wadt, W. R.; Hay, P. J. *J. Chem. Phys.* **1985**, *82*, 284–298.

(32) Schaftenaar, G.; Nordik, J. H. *J. Comput.-Aided Mol. Design* **2000**, *14*, 123–134.

(33) Program Mercury is available at no cost from www.ccdc.cam.ac.uk/products/mercury

Table of Content Graphic.

